CHAPTER 11

BIOGEOCHEMICAL, MINERALOGICAL, AND HYDROLOGICAL CHARACTERISTICS OF AN IRON REACTIVE BARRIER USED FOR TREATMENT OF URANIUM AND NITRATE

Baohua Gu*, David B. Watson, Debra H. Phillips, and Liyuan Liang

Chapter 11 in

Groundwater Remediation of Trace Metals, Radionuclides, and Nutrients, with Permeable Reactive Barriers. D. L. Naftz, S. J. Morrison, J. A. Davis, C. C. Fuller, eds. Academic Press. pp305-342.

* Corresponding author. Phone: 865-574-7286; Fax: 865-576-8543; e-mail: gub1@ornl.gov

Environmental Sciences Division, Oak Ridge National Laboratory, P.O. Box 2008, Oak Ridge, TN 37831.

ABSTRACT

A permeable iron reactive barrier was installed in late November, 1997 at the U.S. Department of Energy's Y-12 National Security Complex in Oak Ridge, Tennessee. The overall goal of this research was to determine the effectiveness of the use of zero-valent iron (Fe^0) to retain or remove uranium and other contaminants such as technetium and nitrate in groundwater. The long-term performance issues were investigated by studying the biogeochemical interactions between Fe^0 and groundwater constituents and the mineralogical and biological characteristics over an extended field operation. Results from nearly 3 years of monitoring indicated that the Fe^0 barrier was performing effectively in removing contaminant radionuclides such as uranium and technetium. In addition, a number of groundwater constituents such as bicarbonates, nitrate, and sulfate were found to react with the Fe^0. Both nitrate and sulfate were reduced within or in the influence zone of the Fe^0 with a low redox potential (i.e., low Eh). An increased anaerobic microbial population was also observed within and in the vicinity of the Fe^0 barrier, and these microorganisms were at least partially responsible for the reduction of nitrate and sulfate in groundwater. Decreased concentrations of Ca^{2+} and bicarbonate in groundwater occurred as a result of the formation of minerals such as aragonite ($CaCO_3$) and siderite ($FeCO_3$), which coincided with the Fe^0 corrosion and an increased groundwater pH. A suite of mineral precipitates was identified in the Fe^0 barrier system, including amorphous iron oxyhydroxides, goethite, ferrous carbonates and sulfides, aragonite, and green rusts. These minerals were found to be responsible for the cementation and possibly clogging of Fe^0 filings observed in a number of core samples from the barrier. Significant increases in cementation of the Fe^0 occurred between two coring events conducted at ~1 year apart and appeared to correspond to the changes in an apparent decrease in hydraulic gradient and connectivity. The present study concludes that, while Fe^0 may be used as an effective reactive medium for the retention or degradation of many

redox-sensitive contaminants, its long-term reactivity and performance could be severely hindered by its reactions with other groundwater constituents; and groundwater flow may be restricted because of the build up of mineral precipitates at the soil/Fe^0 interface. Depending on the site biogeochemical conditions, the rate of Fe^0 corrosion may increase; therefore, the life span of the Fe^0 barrier could be shorter than predicted in previous studies (~15–30 years).

I. INTRODUCTION

The use of zero-valent iron (Fe^0) filings to remediate groundwater contaminated with chlorinated organic compounds, heavy metals, and radionuclides has received considerable attention in recent years (Gillham et al., 1994; Gu et al., 1999; Liang et al., 2000; O'Hannesin and Gillham, 1998; Puls et al., 1999; Scherer et al., 2000; Sivavec et al., 1997; Tratnyek et al., 1997). Although the mechanisms for degrading or immobilizing these contaminants with Fe^0 are not completely understood (Roberts et al., 1996; Sivavec et al., 1997), it has been shown that Fe^0 is a promising reactive medium because of its efficiency in degrading or retaining contaminants and its relatively low cost. Consequently, the Fe^0–based reactive barrier treatment has been widely emplaced for passive, long-term applications for groundwater remediation.

While the focus of many applications was on utilizing an Fe^0–based barrier treatment system to remove or retain environmental contaminants, relatively few studies have paid particular attention to other biogeochemical reactions that may occur simultaneously as Fe^0 corrodes in groundwater. It is recognized that groundwater geochemistry plays a significant role in determining rates of Fe^0 corrosion, its surface reactivity, mineral precipitation and/or barrier clogging, microbial activity, and consequently the long-term performance of the Fe^0 treatment system (Gu et al., 1999; Liang et al., 2000; Scherer et al., 2000). Although the roles of dissolved O_2 and pH in determining Fe^0 reactivity and precipitation chemistry are well established, interactions between Fe^0 and other groundwater constituents, such as HCO_3^-, NO_3^-, SO_4^{2-}, and some metal cations, such as Ca^{2+}, are less well studied and defined. In particular, because SO_4^{2-}, NO_3^-, and HCO_3^- are all corrosive to Fe^0 (Agrawal et al., 1995; Gui and Devine, 1994; Lipczynska-Kochany et al., 1994; Odziemkowski et al., 1998) and are commonly found in groundwater at contaminated sites, these groundwater constituents are of great significance in

influencing both the geochemical and biological interactions and the barrier-clogging processes.

A potential limitation of the Fe^0 technology is the deterioration of the Fe^0 reactive media by corrosion and the subsequent precipitation of minerals that may cause cementation and decreased permeability of the Fe^0 barrier or the surrounding soil. Few studies are available concerning the mineralogical and long-term performance characteristics of Fe^0-based barriers (Gu et al., 1999; Mackenzie et al., 1997; O'Hannesin and Gillham, 1998). However, data indicate that a suite of mineral precipitates can occur rapidly in the Fe^0 barrier system, and flow restriction could occur under certain biogeochemical conditions (Gu et al., 1999; Liang et al., 1997; Mackenzie et al., 1997; Phillips et al., 2000). Minerals such as goethite, magnetite, ferrous carbonates, sulfides, green rusts, and calcite have been reported in both laboratory and field investigations (Gu et al., 1999; Phillips et al., 2000; Pratt et al., 1997). For example, a substantially decreased flow rate was observed over a 6-month period in a series of Fe^0-filled canisters used for treating trichloroethylene-contaminated groundwater at the Portsmouth Gaseous Diffusion Plant (Piketon, Ohio) (Liang *et al.* 1997). Post-treatment analysis of the Fe^0 filings showed cementation of the iron grains, possibly as a result of precipitation of iron sulfides, oxyhydroxides, and carbonates. Clogging also has been reported in laboratory and pilot-scale studies with Fe^0 filings as reactive media (Johnson and Tratnyek, 1994; Scherer et al., 1998). At the Lowry Air Force base (AFB) in Denver, CO, and at Elizabeth City, NC, sites, green rusts (i.e., a mixture of partially reduced/oxidized iron oxyhydroxides and sulfate) were observed in barrier materials (Edwards et al., 1996; Puls et al., 1999). At the Hill AFB, Utah, site, precipitation of iron and calcium carbonates was concluded to be responsible for a 14% porosity reduction within a few months of operation (Shoemaker et al., 1995). In contrast, mineral precipitation was not observed after one year of operation in a reactive barrier at the

Borden, Ontario, site.

This chapter presents the results obtained from ~3 years of groundwater monitoring to evaluate the performance of an Fe^0 reactive barrier used primarily for the retention (or degradation) of uranium (U) and other contaminants such as technetium (Tc) and nitrate (NO_3^-) at the U.S. Department of Energy's Y-12 National Security Complex in Oak Ridge, Tennessee. Emphasis was given to the biogeochemical interactions between Fe^0 and groundwater constituents, the mineralogical and hydrological characteristics, and related long-term performance issues of the reactive barrier system.

II. BARRIER SITE DESCRIPTION

II.A. Site Hydrogeology

Past waste disposal activities at the Oak Ridge Y-12 S-3 ponds have created a mixed-waste plume of contamination in the underlying unconsolidated residuum and competent shale bedrock. The plume is more than 400 ft deep directly beneath the ponds and extends ~4,000 ft along geologic strike both east and west of the ponds. The S-3 ponds consisted of four unlined ponds constructed in 1951 on the west end of the Y-12 Plant. The ponds had a storage capacity of 40 million liters (or ~10 million gallons). Liquid wastes, composed primarily of nitric acid plating wastes, containing various metals and radionuclides (e.g., Ni, Cr, U, and Tc) were disposed of in the ponds until 1983. Volatile organic compounds such as tetrachloroethylene and acetone also were disposed in the ponds, although only low levels of chlorinated organic contaminants and acetone were detected in the groundwater at the barrier site. Pond wastes that remained were neutralized and denitrified in 1984, and the site was capped and paved thereafter (Cook et al., 1996; SAIC, 1996, 1997).

The geology that underlies the site is primarily the Nolichucky shale bedrock that dips approximately 45 degrees to the southeast and has a strike of N55E (parallel to Bear Creek Valley). Overlying the bedrock is unconsolidated material that consists of weathered bedrock (referred to as residuum or saprolite), alluvium, colluvium, and man-made fill materials. Silty and clayey residuum comprises most of the unconsolidated material in this area. The residuum overlying the Nolichucky shale is typically between 5 and 10 m (~20 and 30 ft) thick. Between the unconsolidated residuum and competent bedrock is a transition zone of weathered fractured bedrock. Remnant fracturing in the residuum and transition zone increases the permeability relative to the silt and clay matrix. The shallow groundwater flow direction west of the S-3 Ponds is generally to the southeast with a horizontal gradient of approximately 0.016 ft/ft (SAIC, 1996). Additionally, upward vertical hydraulic gradients were identified at the site and are as high as 0.25 ft/ft between the competent bedrock and transition zone, and ~0.12 ft/ft between the transition zone and shallow unconsolidated zone (Watson et al., 1999).

In general, the groundwater plume near the S-3 ponds is composed primarily of nitrate, bicarbonate, uranium, technetium, and other metal ions. These inorganic metal contaminants include low levels of heavy metals such as Ni, Cr, Co, Cd, Zn, and Pb. The plume is stratified, with the distribution of contaminants dependent on geochemical characteristics of the contaminants and groundwater. For example, nitrate and technetium (as pertechnetate, TcO_4^-), which are not particularly reactive with soil minerals, have the most extensive distribution in groundwater. Uranium and heavy metals that are more reactive are not as deep and have not migrated as extensively away from the ponds. Three major groundwater migration pathways to Bear Creek and its tributaries have been identified during the Bear Creek Valley Treatability Study (SAIC, 1997).

- Pathway 1 is located just to the south of and adjacent to the S-3 Ponds and is a shallow pathway to the upper reach of the Bear Creek. Contaminants in this pathway include uranium, technetium, nitrate, metals, and high total dissolved solids (TDS).
- Pathway 2 is another shallow pathway to the upper reaches of Bear Creek and is located approximately 600 ft downstream west from Pathway 1. This pathway is thought to be associated with an old burial Bear Creek stream channel. The iron/gravel trench barrier is located at this site and is targeted to treat primarily low levels of uranium and nitrate (described in detail in Section II.B).
- Pathway 3 consists of contaminated groundwater in bedrock that is migrating to the west along strike in the Nolichucky Shale. Contaminants in this deeper pathway discharge to tributaries of Bear Creek and include technetium, nitrate, metals, and high TDS. Pathway 3 contains much less uranium than the other pathways.

II.B. Installation of the Iron-Gravel Trench Barrier

A permeable iron-gravel trench barrier was constructed at the Pathway 2 site in late November 1997 as part of the technology demonstration using Fe^0 to retain or remove uranium and other contaminants as groundwater passively passes through the Fe^0 treatment medium. The Pathway 2 site is predominantly a shallow pathway for the migration of uranium-contaminated groundwater (~1 mg/L) to the upper reach of Bear Creek. The nitrate concentrations are generally lower (~20–150 mg/L) at Pathway 2 than other areas of the groundwater plume, but they have been detected at levels above 1000 mg/L in some of the deeper piezometers because of the upward vertical hydraulic gradient. Technetium is generally detected at levels below 600 pCi/L, and TDS concentrations (~1000 mg/L) are generally lower than in the shallow plume at

pathway 1 and deeper parts of the S-3 plume. Uranium-contaminated groundwater is discharging to the creek near Pathway 2 through seeps adjacent to the headwaters of Bear Creek.

The trench dimensions are ~225 ft in length, 2 ft in width, and ~30 ft in depth (to bedrock) with an Fe^0-filled midsection of ~26 ft in length between two ~100-ft sections of granite/quartz-pea gravel (Figure 1). Guar-gum biopolymer slurry was used during trench excavation to prevent the walls from collapsing, and Peerless Fe^0 filings (about –1/2 to 25 mesh size, from Peerless Metal Powders and Abrasives, Detroit, Michigan) were used as the reactive medium in the midsection of the barrier. A total of ~80 tons of Peerless iron filings was placed in the middle section of the trench to a depth of ~18–20 ft above the bottom of the trench, or 10 to 12 ft below original ground surface. The sediments around the barrier are heterogeneous mixtures of fill materials, native soil, saprolite, and rock fragments (Watson et al., 1999). Undisturbed soil and saprolite from the Nolichucky Shale formation are present near the bottom of the barrier. The barrier trench is oriented nearly parallel (or in a small angle) to the direction of groundwater flow and was designed to direct groundwater flow through the iron treatment zone using both the natural groundwater gradient and the permeability contrast between the iron/gravel in the trench and the native silt/clay outside the trench. Hydraulic monitoring at the site indicated that the hydraulic gradient is ~0.025 ft/ft across the site but this gradient flattens to 0.01 ft/ft in the vicinity of the barrier trench. Approximately 48 piezometers, including 6 multi-port wells in the Fe^0 barrier, were installed at the site (Figure 1). Additional information regarding the site and its hydrogeology has been reported elsewhere (Phillips et al., 2000; Watson et al., 1999).

After completion of the trench installation, the bio-polymer Guar gum was broken down with an enzyme (LED-4 jell breaker, GeoCon, Inc.) that was circulated through the trench for 2

days. That process was followed by a 5-day step-drawdown pumping test and a 7-day pumping test in the trench. The primary purpose of these initial pumping tests was to determine the hydraulic conductivity and groundwater flow conditions for a remediation scenario at the site.

II.C. Groundwater and Core Sampling and Analysis

Periodic groundwater samples were collected for the determination of contaminant metals/radionuclides (e.g., U, Tc, Cr), geochemical parameters [e.g., major cations and anions, pH, Eh, dissolved oxygen (DO), and total organic carbon (TOC)], and microbial characteristics from some selected monitoring wells. The groundwater pH, Eh, DO, and temperature were measured in line (without exposing to the air) by means of a YSI XL600M multiparameter probe (Yellow Springs Instruments, CO), which had been pre-calibrated. Ferrous ion (Fe^{2+}) and sulfide (S^{2-}) were determined immediately after taking samples in the field by the colorimetric technique using HACH kits equipped with a DR/2000 spectrophotometer (HACH, Loveland, CO).

The filtered groundwater samples (using 0.45-μm in-line filters) were also collected in two separate containers, either acidified or unacidified with concentrated nitric acid. The acidified samples were used for elemental analysis such as Ca, Mg, Fe, Al, Mn, Ni, Cd, Cr, Cu, Pb, Zn, Co, Sr, Na, K, and Si by inductively coupled plasma – atomic emission spectroscopy (Thermo Jarrell Ash PolyScan Iris Spectrometer). The unacidified samples were used for the analysis of major anions including nitrate (NO_3^-), sulfate (SO_4^{2-}), chloride, and phosphate by means of an ion chromatograph equipped with a conductivity detector (Dionex, Sunnyvale, CA). Aliquots of the unacidified samples were also used for the analyses of TOC and total inorganic carbon (TIC) by means of a total organic carbon analyzer (TOC–5000A, Shimadzu, Tokyo). The TIC was then converted to bicarbonate (HCO_3^-) or carbonate concentrations in groundwater.

An aliquot of the acidified groundwater sample was also used for the analysis of total U(VI) by means of a laser-induced kinetic phosphorescence analyzer (ChemChek, KPA-11). However, because of a relatively low U(VI) concentration and the interference (or quenching effects) of other groundwater constituents such as Cl^- and Ca^{2+} in groundwater, the samples were purified and preconcentrated using the UTEVA resin extraction columns (Eichrom, IL). Experimentally, an aliquot of groundwater sample (10–20 mL) was acidified with nitric acid to a minimum concentration of 3 M, in which uranyl (UO_2^{2+}) forms complexes with NO_3^- (Horwitz et al., 1992). The uranyl-nitrate complexes were subsequently sorbed by the UTEVA resin, leaving other groundwater constituents unsorbed (or in the leachate). The column was then leached with dilute HNO_3 (1 mM), in which uranyl-nitrate complexes are unstable (or dissociate) and therefore desorbed from the resin column. The dilute HNO_3 leachate (with uranium) was collected and analyzed for U(VI) content as described above, and the detection limit was better than 0.01 μg/L.

About 1.2 and 2.5 years after the Fe^0 barrier was installed, soil and iron core samples were collected in polyurethane tubes from the barrier and its adjacent fill materials and used for the analyses of surface morphology, mineral precipitation, uranium content, and microbial characteristics. The mineralogical characterization of the core materials was performed using X-ray diffraction (XRD) operated at 45 kV and 40 mA (Scientag XDS–2000 diffractometer, Sunnyvale, CA). To determine the mineral deposition, morphology, and elemental composition, the Fe^0 core samples were also carbon-coated with a Bio-Rad carbon sputter coater and immediately examined by means of a JEOL ISM-35CF scanning electron microscope (SEM) equipped with an energy dispersive x-ray analyzer (EDX) (Tokyo, Japan). Note that all core samples were stored in Ar-purged airtight PVC tubes before use so as to minimize oxidation.

Additionally, it is pointed out that the sample preparation and timing are critical because such minerals as green rusts are particularly sensitive to oxidation and drying methodologies, and details regarding sample preparation and analytical procedures can be found elsewhere (Gu et al., 2001; Phillips et al., 2001; Phillips et al., 2000).

III. BIOGEOCHEMICAL REACTIONS IN THE IRON REACTIVE BARRIER

Although the ultimate goal of constructing the Fe^0 reactive barrier is to retain or degrade target contaminants of concern in groundwater, it must be realized that a range of biogeochemical reactions occur simultaneously because Fe^0 reacts not only with contaminant chemicals but also with a number of natural groundwater constituents. As illustrated in Figure 2, corrosion of Fe^0 in groundwater generates soluble Fe^{2+} ions, dissolved H_2, and an increased groundwater pH. More important, corrosion of Fe^0 results in a low redox potential (or Eh) and provides excess electrons for the reduction of a number of redox-sensitive contaminant metal species (e.g., uranyl, pertechnetate, and chromate), chlorinated organic compounds, and other groundwater constituents (e.g., nitrate and sulfate). Depending on the site biogeochemical conditions, these reactions are of great importance because they not only affect on the reactivity and long-term performance of Fe^0 to retain or remove contaminants, but also determine the rate of Fe^0 corrosion and, hence, the life span of the permeable Fe^0 reactive barrier.

III.A. Groundwater pH, Eh, and Ferrous Ion

Corrosion of Fe^0 in groundwater follows two general pathways. In the presence of dissolved oxygen, Fe^0 corrodes according to the reaction

$$Fe^0 + H_2O + \frac{1}{2}O_2 \rightarrow Fe^{2+} + 2OH^- . \qquad (1)$$

However, under anaerobic conditions (e.g., oxygen consumed by the above reaction or by anaerobic microorganisms), Fe^0 can react with water according to:

$$Fe^0 + 2H_2O \rightarrow Fe^{2+} + H_2 + 2OH^- . \quad (2)$$

Both of these reactions result in a decreased redox potential but an increased solution pH as 2 moles of OH^- are formed per mole of Fe^0 oxidized. As shown in Figure 3, the site groundwater pH (upgradient) is generally stabilized at ~6.5. However, upon reaction with Fe^0 in the barrier, groundwater pH within the Fe^0 increased and stabilized at from ~7.5 up to ~10 under field conditions. On the other hand, groundwater pH remained at ~6.5 in downgradient wells (except those in the Fe^0 barrier, DP-23s,m), and corrosion of Fe^0 in the barrier appeared to have little impact on the downgradient soil based on observed pH values (Figure 3). This observation may be attributed to the relatively high pH-buffering capacity of clay minerals and organic matter in downgradient soil. The groundwater pH in monitoring well from TMW-7 appeared to be somewhat high (up to ~9.5) because this well is situated in the gravel trench downgradient of the Fe^0 barrier, that is low in pH-buffering capacity.

Groundwater redox potential (Eh), however, decreased dramatically in those monitoring wells both within and downgradient of the Fe^0 barrier (Figure 4). Although the site groundwater is generally aerobic, with Eh values mostly positive (over +200 mV) (Figure 4 upgradient), a generally low Eh was observed within the Fe^0 barrier (<–200 mV). This decrease in Eh may directly result from the consumption of dissolved O_2 and the production of dissolved H_2 as groundwater reacted with Fe^0 in the reactive zone. The Eh values were also in the negative range in most of the downgradient monitoring wells. Note that a low Eh was also observed in the upgradient TMW-11 and DP-22s monitoring wells because the DP-22 well is also located within the Fe^0 barrier and the TMW-11 is located adjacent to the Fe^0 barrier. The use of Guar gum

could also have resulted in an increased anaerobic microbial activity (Gu et al., 2001) and thus may have contributed to a low redox potential in the TMW-11 monitoring well.

Ferrous iron (Fe^{2+}), one of the major byproducts of Fe^0 corrosion in groundwater, may have a significant impact on water quality and cause clogging of soil porous structure as it oxidizes and precipitates out in the downgradient barrier or the soil. In fact, discharge of Fe^{2+} to Bear Creek had been one of the major concerns initially regarding the implementability of Fe^0 barriers at the site. However, we found that Fe^{2+} concentrations in groundwater were relatively low after a few months of operation of the Fe^0 barrier in the field (Figure 5). Initially, the Fe^{2+} concentration was found to be extremely high (up to ~150 mg/L) in the center well (TMW-9) of the Fe^0 barrier, and total iron concentration reached levels as high as ~700 mg/L (data not shown). Relatively high Fe^{2+} concentrations were also observed in the pea gravel section adjacent to the Fe^0 barrier for TMW-7 and TMW-11 (Figure 6). However, Fe^{2+} concentrations decreased rapidly over the first few months after the Fe^0 barrier was installed (such as in the TMW-9 and TMW-7 wells). Only a few monitoring wells within the Fe^0 barrier showed a slightly high Fe^{2+} concentration but was <15 mg/L in general (e.g., DP-22s,m; DP-20s,m; DP-23s) (Figure 5). As will be discussed below, Fe^{2+} ions may be precipitated as FeS, $FeCO_3$, or be further oxidized as Fe^{3+}, which forms relatively insoluble iron oxyhydroxides in the Fe^0 barrier. These results suggest that Fe^{2+} discharge as a result of Fe^0 corrosion is not always a significant concern at this site. However, the rate of Fe^0 corrosion and the production of Fe^{2+} will depend on both groundwater pH and constituent concentrations, such as nitrate, sulfate, and bicarbonate, which accelerate the corrosion process (Agrawal and Tratnyek, 1996; Agrawal et al., 1995; Gu et al., 1999). Depending on the removal rates via precipitation and sorption, high concentrations of ferrous ion may persist under certain conditions.

The high initial Fe^{2+} and total iron concentrations observed in groundwater (Figure 5) may be attributed in part to the following factors: (1) a rapid initial oxidation of Fe^0 filings (particularly some fine iron particles) when they were emplaced into the groundwater; 2) the use of Guar gum and, subsequently, the addition of enzyme (used to break up the Guar gum), that resulted in a decreased groundwater pH in a short time period; and (3) increased microbial activity (or respiration), which may also contribute to an increased corrosion rate of Fe^0.

III.B. Reactions Between Nitrate and Fe^0

Groundwater at the barrier site is contaminated with relatively high levels of nitrate (NO_3^-) at ~20–150 mg/L at the Pathway 2 site; in some deep monitoring wells or piezometers, levels >1000 mg/L NO_3^- were observed as a result of the migration of deep contaminated groundwater and the upward vertical hydraulic gradients at the site. Within and in the vicinity of the Fe^0 barrier, however, the NO_3^- concentration were low to non-detectable (Figure 7), suggesting that NO_3^- was effectively degraded as the groundwater passed through the Fe^0 barrier. The nitrate concentrations were also found to be low or non-detectable downgradient of the Fe^0 barrier, including monitoring wells or piezometers TMW-7, DP-11, DP-14s, DP-15s, and many others that are not shown in Figure 6. Even in some upgradient monitoring wells or piezometers (adjacent to the Fe^0 barrier), a low NO_3^- concentration was observed in monitoring wells such as TMW-11 and DP-12. These observations suggest that NO_3^- is readily degraded in the reducing zone of influence by Fe^0 corrosion.

The reduction of NO_3^- observed in the downgradient and some upgradient monitoring wells may be partially attributed to denitrification by microorganisms. As reported previously (Gu et al., 2001), an enhanced anaerobic microbial population was observed in soils both downgradient and upgradient of the Fe^0 barrier. This was presumably related to a low Eh and an

increased level of dissolved H_2 in groundwater (a byproduct of Fe corrosion), which served as electron donors for the microbial reduction of NO_3^-. However, direct abiotic reduction of NO_3^- by Fe^0 filings should not be ruled out within the Fe^0 barrier (Gu et al., 1997; Huang et al., 1998).

In laboratory, the reduction of NO_3^- and its associated byproducts by Fe^0 filings was evaluated in the presence or absence of peat materials and/or denitrifying bacteria. Results indicated that nitrate was effectively reduced by Fe^0, despite a relatively high initial NO_3^- concentration (6000 mg/L) used in these laboratory batch experiments (Figure 7a). The degradation half-life by Fe^0 alone was found to be on the order of ~1–2 weeks by assuming a pseudo-first-order reaction kinetics, and more than 60% of NO_3^- was degraded after about 2 weeks of reaction. The addition of peat materials (from Wards Scientific) was found to enhance the reduction rate of NO_3^-, with a decreased reaction half-life on the order of ~2 days. More than 95% of the NO_3^- was degraded in a 1-week period. However, note that the reduction rates did not increase significantly with the addition of a toluene-degrading denitrifying bacterium, *Azoarcus tolulyticus* Tol-4, into the Fe^0 and peat mixture (Chee-Sanford et al., 1996). In fact, addition of this denitrifying bacterium directly into Fe^0 filings did not increase the denitrification either, probably because of a high NO_3^- concentration and a relatively high pH condition (up to ~10) in the reactant solutions or an unfavorable environment for microbial reduction of NO_3^-. The presence of peat (with indigenous microbes in the peat), however, buffered the pH of the reactant solution (pH <8.5) so that a substantially enhanced NO_3^- reduction rate was observed under these conditions. Nevertheless, results of these laboratory experiments are consistent with the field monitoring results and demonstrate that Fe^0 is an effective reactive medium for removing NO_3^-, in addition to degrading chlorinated organics and sequestering some redox-

sensitive metals or radionuclides, as reported previously (Blowes et al., 1997; Cantrell et al., 1995; Gillham et al., 1994; Gu et al., 1998; McMahon et al., 1999).

The reaction byproducts between NO_3^- and Fe^0 and peat mixtures were also examined. The results (Figure 7b) indicate that a portion of NO_3^- (~25%) was converted to ammonia (NH_4^+) in the aqueous solution, and a large percentage of NO_3^- may have been degraded as N_2 or N_2O gases. A good mass balance was not obtained in these batch kinetic experiments, largely because of the loss of N_2 and N_2O gases to the headspace or atmosphere.

III.C. Sulfate Reduction

A decreased concentration of sulfate (SO_4^{2-}) also was observed within the Fe^0 barrier. As illustrated in Figure 8, sulfate was the highest in the upgradient soil and pea gravel portion of the barrier. Upon entering the Fe^0 portion of the trench, sulfate was found to be substantially reduced at all levels. For example, at the multi-level monitoring wells of DP-19 and DP-20, the SO_4^{2-} concentrations were significantly lower than those in the upgradient wells. In particular, sulfate was largely removed or degraded in some of the downgradient monitoring wells in soil (e.g., DP-14s), in iron (DP-23s,m), and in gravel (TMW-7). These observations provide evidence of sulfate reduction in the zone of Fe^0 influence, although the mechanisms of sulfate reduction are still a subject of investigation. These observations are also consistent with previous studies that show that groundwater SO_4^{2-} concentrations decreased through the Fe^0 barriers at the Moffett Field and Lowry AFB sites, at the Elizabeth City, U.S. Coast Guard site (Puls et al., 1999), and in the laboratory-simulated column studies with a continuous input of SO_4^{2-} and HCO_3^- solutions (Gu et al., 1999).

The reduction of SO_4^{2-} resulted in the formation of sulfide (S^{2-}), although much of the sulfide produced may have been rapidly precipitated as FeS because of its low solubility (K_{sp} on

the order of 10^{-18}). This explains a relatively low S^{2-} concentration observed in most of the monitoring wells (data not shown). Nevertheless, sulfide concentrations were found to be somewhat higher in those monitoring wells adjacent to the iron (TMW-11 and TMW-7) and within the iron barrier (TMW-9) than in those monitoring wells upgradient of the Fe^0 barrier (TMW-12 and DP-12). The exact mechanism of SO_4^{2-} reduction to S^{2-} is not yet clear because there is no direct evidence showing an abiotic reduction of SO_4^{2-} by Fe^0, although reduction of sulfonic acid to S^{2-} by Fe^0 has been reported (Lipczynska-Kochany et al., 1994). However, a decreased SO_4^{2-} concentration in the barrier could be at least partially attributed to reduction by sulfate-reducing microorganisms (Gu et al., 2001).

Using phospholipid fatty acids (PLFA) and DNA analyses (Dowling et al., 1986; Guckert et al., 1986; Tunlid and White, 1991; Zhou et al., 1996), an increased microbial population was observed within and in the vicinity of the Fe^0 barrier. The microbial population was found to be on the order of 10^5 to 10^6 cells/mL groundwater, which is substantially higher than that found in the background soil, located ~50 ft upgradient of the Fe^0 barrier (Gu et al., 2001). More importantly, perhaps, diversified microbial communities were also detected in groundwater by examining the characteristic PLFA profiles or lipid biomarkers although PLFA analysis is unable to identify the specific functional groups of microorganisms. Many microbial species may have similar PLFA patterns. Therefore, DNA analysis based on polymerase chain reactions (or PCR analysis) was used to further identify different functional groups of microorganisms. As reported previously, sulfate-reducing bacteria appeared to be one of the most abundant microorganisms identified in both groundwater and core samples obtained within and in the vicinity of the Fe^0 barrier. Both sulfate-reducing and denitrifying bacteria were found to be the highest in TMW-11 (upgradient adjacent to the Fe^0 barrier) and DP-11 (~3 ft downgradient of the Fe^0 barrier). These

observations provide additional evidence that a decreased SO_4^{2-} concentration within the Fe^0 portion of the trench could be a result of microbial reduction of SO_4^{2-} to S^{2-} under anaerobic conditions. Hydrogen generated by the corrosion of Fe^0 (and the initial use of Guar gum for trench excavation) could have played a significant role in stimulating the growth of these anaerobic microorganisms (Gu et al., 1999).

III.D. Interactions Between Fe^0 and Contaminant Metals

III.D.1. Uranium Removal

At the Y-12 site, uranium is the main driver for this groundwater remediation using the permeable Fe^0 reactive barrier because uranium poses the major potential health and environmental risks within Bear Creek Valley. Its concentration trends within and in the vicinity of the Fe^0 barrier are plotted in Figure 9 for some monitoring wells and piezometers. Results indicate that uranium is effectively removed within the Fe^0 barrier, and that uranium concentrations in the Fe^0 barrier (e.g., TMW-09, DP-19s,m, and DP-20s,m) were generally very low (<0.01 mg/L) in comparison with uranium concentrations in the upgradient monitoring wells. Low amounts of uranium were also found in the downgradient wells (e.g., DP-23s,m, DP-10, and DP-14s, TMW-7), suggesting that the Fe^0 barrier is performing well in removing or retaining uranium from the contaminated groundwater. Similarly, uranium concentrations in other monitoring wells and piezometers (such as DP-18s,m,d; DP-21s,m; DP-22s) were found to be low or below the detection limit in the Fe^0 barrier (data not shown). These observations are therefore consistent with previous laboratory studies that show uranium can be effectively and rapidly reduced by Fe^0 filings (Gu et al., 1998).

Uranium retention by Fe^0 filings was also evidenced by the analysis of uranium content in Fe^0 core samples (Figure 10). These angled cores were collected ~15 months after installation

of the Fe^0 barrier, and detailed sample preparation and analysis were given elsewhere (Phillips et al., 2000). Although only trace quantities of uranium are present in the contaminated groundwater, an elevated amount of uranium was detected in the Fe^0 core materials, particularly in those samples near the interface (between the soil and Fe^0 filings) where groundwater enters the Fe^0 barrier. The greatest concentration of uranium in the Fe^0 barrier occurred at the shallow, upgradient interface, but uranium concentration decreased dramatically over a short distance. These observations suggest that once uranium enters the Fe^0 reactive barrier it is rapidly sequestered in situ as a result of either reductive precipitation of relatively insoluble U(IV) species or surface adsorption of U(VI) species on the Fe^0 corrosion products (e.g., iron oxyhydroxides) (Cantrell et al., 1995; Gu et al., 1998).

Reductive precipitation of U(VI) to U(IV) species by Fe^0 is believed to be one of the dominant mechanisms for uranium removal and is thermodynamically favorable, according to the following stoichiometric reactions (Baes and Mesmer, 1976; Gu et al., 1998; Morse and Choppin, 1991):

$$Fe^{2+} + 2e^- \rightarrow Fe(0) \qquad \varepsilon^o = -0.440 \text{ V} \qquad (3)$$

$$UO_2^{2+} + 4H^+ + 2e^- \rightarrow U(IV) + 2H_2O \qquad \varepsilon^o = +0.327 \text{ V} \qquad (4)$$

$$\text{or} \qquad \varepsilon = -0.07 \text{ V at pH 8.}$$

The reduced U(IV) readily forms oxyhydroxide precipitates in aqueous solution. Such a reductive reaction mechanism has been evaluated by laboratory batch equilibrium studies and by sensitive fluorescence spectroscopic analysis (Gu et al., 1998). The fluorescence spectra gave direct evidence of U(VI) reduction by Fe^0 because the reduced U(IV) species do not fluorescence. The batch equilibrium studies provided additional evidence because, regardless of the initial added uranium concentration in solution (up to 20,000 mg/L), no detectable amounts of uranium were found in the equilibrium solutions after reaction with Fe^0. These results are

indicative of reductive precipitation process rather than a simple sorption process, in which uranyl distributes or partitions between the solution and solid phases depending on the adsorption affinity and capacity on the adsorbent surfaces. On the other hand, sorption by iron oxides and other adsorbent materials was found to be much less effective than Fe^0 filings in removing uranium from the solution. A much higher-equilibrium U(VI) concentration was observed in samples treated with these materials than in those treated with Fe^0 filings. Using the X-ray photoelectron spectroscopy (XPS) technique, Fiedor et al. (1998) also reported that U(VI) was readily reduced to U(IV) species (~75%) by reacting with an Fe^0 coupon under anaerobic conditions, although a large solution to Fe^0 ratio was used in these laboratory studies.

However, as the corrosion products of Fe^0, such as iron oxyhydroxides, accumulate on Fe^0 surfaces, uranium removal through sorption or co-precipitation could not be ruled out (Fiedor et al., 1998; Gu et al., 1998; Hsi and Langmuir, 1985; Morrison et al., 1995). Unfortunately, because of a relatively low amount of uranium retained by the Fe^0 filings and a possible reoxidation of reduced U(IV) species during sample preparation and extraction, no attempts were made to distinguish whether uranium was reductively precipitated or sorbed by iron oxyhydroxides in these Fe^0 barrier materials. On the basis of previous laboratory studies (Cantrell et al., 1995; Fiedor et al., 1998; Gu et al., 1998), a speculation is that a majority of uranium could have been retained by the reductive precipitation process because of a strong reducing environment within the Fe^0 barrier (with a high solid to solution ratio). Understanding of U(VI) removal mechanisms through either reductive precipitation or sorption/co-precipitation has important environmental implications because the reduced U(IV) species on Fe^0 surfaces could be potentially re-oxidized when it is exposed to the air or dissolved O_2 in a matter of a few

hours or days (Gu et al., 1998). Similarly, the sorbed U(VI) species could be desorbed and therefore remobilized as groundwater geochemistry changes.

III.D.2. Pertechnetate and Chromate Reduction

The effectiveness of the Fe^0 barrier in removing other contaminant metals such as pertechnetate (TcO_4^-) and chromate (CrO_4^{2-}) was also monitored, although they are not major contaminants of concern because of their low concentration in the site groundwater. Technetium (as TcO_4^-) is a radioactive β-emitter with an extremely long half-life (2.1 x 10^5 years), and chromate is a hazardous heavy metal. Results indicate that TcO_4^- was also effectively retained by the Fe^0 barrier and that generally less than 40 pCi/L (or ~2 ng/L) of ^{99}Tc was detected in those monitoring wells within or adjacent downgradient of the Fe^0 barrier. The influent groundwater (in upgradient monitoring wells) contained ~600 pCi/L of TcO_4^-. The chromate concentrations in the upgradient and downgradient groundwater were mostly below the detection limit. As with the U(VI) species, the mechanisms of TcO_4^- and CrO_4^{2-} removal by Fe^0 filings are attributed to a reductive precipitation process, which was confirmed in laboratory batch kinetic studies (Figure 11). As Fe^0 corrodes in water, CrO_4^{2-} can be reduced to Cr^{3+}, which is easily hydrolyzed and precipitated as $Cr(OH)_3$. Similarly, TcO_4^- is reduced to TcO_2 or $Tc(OH)_4$ as precipitates. The reduction kinetics of these contaminant metals or radionuclides appears to be extremely fast, and nearly 100% of UO_2^{2+}, TcO_4^-, and CrO_4^{2-} was removed after they contacted Fe^0 in water in a short time period (Figure 11). The reductive precipitation or removal of CrO_4^{2-} has also been reported previously in the Fe^0 reactive barrier used to remediate groundwater contaminated with CrO_4^{2-} and trichloroethylene at the U.S. Coast Guard site, at Elizabeth City, NC (Blowes et al., 1997; Puls et al., 1999).

III.E. Interactions with Calcium and Carbonates

The groundwater at the barrier site contains high concentrations of both Ca^{2+} and bicarbonate because of the presence of calcium-rich bedrock, the calcareous Nolichucky shale, and strong nitric acid leachate from the S-3 Ponds, and because of the neutralization of the acid wastes by limestone in 1984. An analysis of groundwater carbonate/bicarbonate and Ca^{2+} indicates that these groundwater constituents were partially retained or precipitated within the Fe^0 barrier (Figures 12 and 13). As shown in Figure 12, Ca^{2+} concentrations in the upgradient side of the Fe^0 barrier (e.g., TMW-11, TMW-12, DP-12 and DP-13) appeared to be relatively constant (between ~120 and 200 mg/L). However, the Ca^{2+} concentrations within the Fe^0 barrier from TMW-9, DP-19, and DP-20 monitoring wells were about an order of magnitude lower than those found in the upgradient monitoring wells, suggesting that Ca^{2+} was retained by the Fe^0 barrier. A relatively low Ca^{2+} concentration also was observed in many of the downgradient monitoring wells (e.g., DP-23s,m, TMW-7, and DP-14s).

Examination of carbonate/bicarbonate concentrations in groundwater revealed that these constituents also were partially removed (Figure 13), suggesting that calcium carbonate precipitation is probably one of the dominant mechanisms responsible for decreased concentrations of Ca^{2+} and bicarbonate in groundwater. These results can be expected because of an increased groundwater pH as Fe^0 corrodes in the barrier and a resulting shift from bicarbonate to carbonate species in the groundwater. As has been reported previously, an increased pH and relatively high concentrations of Ca^{2+} and bicarbonate in the groundwater could have induced the chemical precipitation of Ca-carbonate and/or of a mixture of Fe- and Ca-carbonate and oxyhydroxide coprecipitates (Gu et al., 1999; Phillips et al., 2000). Similarly, by examining the concentration profiles of Mg^{2+} (data not shown), we found that Mg^{2+}

concentration within the Fe^0 barrier also decreased over time because it also could form carbonate precipitates or co-precipitates with iron oxyhydroxides (Phillips et al., 2000).

IV. HYDROLOGICAL AND MINERALOGICAL CHARACTERISTICS

IV.A. Hydraulic Properties and Connectivity in the Fe^0 Barrier

Hydraulic gradients across the Pathway 2 barrier site have remained relatively stable and consistent from east to west (magnitude of approximately 0.02). Figures 14a,b show a comparison of groundwater levels and flow directions on May 6, 1998 and on May 17, 2000, respectively. The results indicate that the general flow patterns at the site have not changed since the start of the installation of the trench. Groundwater monitoring results over the past 3 years also suggest that increases and decreases in the gradients across the reactive barrier site appear to be primarily related to recharge during precipitation events and seasonal fluctuations. The hydraulic gradient in the trench across the iron has also remained consistently from east to west (Figure 14) with an average gradient of approximately 0.008. The magnitude of the gradient changes during recharge events but the direction of groundwater flow has been consistently toward the west. However, closer inspection of gradient fluctuations within the trench and the Fe^0 barrier seem to indicate that cementation within the iron may be starting to impact groundwater flow through the iron. Figure 15 shows the groundwater elevations and gradients between 3 monitoring wells located in the Pathway 2 trench. Since the spring of 1999 (or ~500 days after the barrier was installed), recharge events appear to have a more pronounced impact on hydraulic gradients (or fluctuations) observed between wells located upgradient (TMW-11), within (TMW-9), and downgradient (TMW-7) of the Fe^0 barrier. These observations suggest that the connectivity of the iron and gravel in the upgradient portion of the trench to the iron and

gravel in the downgradient portion of the trench may be decreasing over time due to mineral precipitation and/or cementation in the Fe^0 barrier, as will be discussed in Sections IV.B below. Coincidentally, the nitrate concentrations in upgradient well TMW-11 and DP-22m (located the furthest upgradient but still in the Fe^0 barrier) have an increasing trend starting in the spring of 1999 (Figure 6). These data suggest that cementation of the iron in the upgradient portion of the trench may be causing a decrease in iron reactivity, hydraulic connectivity, and the beginning stages of system clogging.

IV.B. Mineral Precipitates and Their Occurrence

Iron corrosion in groundwater results in the formation of ferrous or ferric ions (when dissolved O_2 is present), which ultimately form iron oxyhydroxide mineral precipitates because of their low solubility (Figure 2). It is not surprising, therefore, that many investigators observed iron oxyhydroxides to be the predominant minerals found in the iron reactive barriers (Gu et al., 1999; Phillips et al., 2000; Pratt et al., 1997; Roh et al., 2000). Core samples were taken ~1.2 and 2.5 years after the Fe^0 barrier was installed, and X-ray diffraction (XRD) analysis revealed akaganeite (β-FeOOH) as the major iron mineral precipitant throughout the cores, while goethite (α-FeOOH) was present to a lesser extent (Phillips et al., 2000). Although they were not detected by the XRD analysis, amorphous iron oxyhydroxide deposits were also observed throughout the iron core materials by means of scanning electron microscope (SEM) and energy dispersive X-ray (EDX) spectroscopic analyses. Presumably, these amorphous iron oxyhydroxides gradually transform to crystalline akaganeite and goethite within the barrier. The formation of akaganeite may be related to a relatively high concentration of chloride in groundwater entering the trench, because, in laboratory studies, akaganeite is commonly

observed as the dominant mineral phase from precipitation of ferric chloride (Schwertmann and Cornell, 1991). The presence of goethite within the Fe^0 barrier instead of lepidocrocite, which has been reported in laboratory column studies (Gu et al., 1999), could result from relatively high dissolved O_2 and bicarbonate contents of the groundwater. It has been reported that the formation of goethite is favored over the formation of lepidocrocite when carbonates or CO_2 are present in the system (Schwertmann and Taylor, 1977).

Although to a lesser extent, green rusts were also observed as corrosion products in the Fe^0 barrier, and similar observations have been reported previously (Gu et al., 1999; Phillips et al., 2000; Roh et al., 2000). However, green rusts are not stable and can transform into crystalline iron minerals quickly when exposed to the air or subjected to oven drying. Therefore, care must be taken in sample preservation and preparation in order to observe green rusts in the iron barrier material (Phillips et al., 2001).

In addition to iron oxyhydroxide minerals, analysis of Fe^0 core materials indicated the presence of abundant calcium carbonates such as aragonite ($CaCO_3$) and siderite ($FeCO_3$) (Figure 16a,b). These results are consistent with decreased concentrations of calcium and carbonates in groundwater within and downgradient of the Fe^0 barrier, as shown in Figures 12 and 13. Crystalline aragonite was observed throughout the core materials of the Fe^0 barrier, and its structure and forms were identified by both SEM and EDX analyses (Figure 16a). As indicated previously, relatively high concentrations of Ca^{2+} and carbonates, coupled with a relatively high pH within the Fe^0 barrier, may be largely responsible for the precipitation of $CaCO_3$ minerals (Phillips et al., 2000; Roh et al., 2000).

The formation of ferrous carbonate (i.e., siderite) offers another mechanism for a decreased carbonate or bicarbonate concentration in the Fe^0 barrier. Ferrous iron is one of the

major byproducts of Fe^0 corrosion in groundwater; it is thus conceivable that the formation of siderite can be a favorable reaction when high amounts of carbonate are present in groundwater, particularly at a relatively high pH condition (Mackenzie et al., 1999). Figure 16b shows the SEM image of cubic-shaped siderite minerals in the Fe^0 barrier. As shown in Figure 13, bicarbonate contents from monitoring wells such as TMW-9 were particularly low and could be attributed largely to its precipitation with both Ca^{2+} and Fe^{2+} to form carbonate minerals. However, siderite precipitation was much less extensive than aragonite precipitation. The presence of siderite was detected only in patches in some of the iron core samples. Several factors may contribute to these observations. A relatively high pH and high carbonate but low Ca^{2+} concentrations favor the formation of siderite (Phillips et al., 2000). On the other hand, a relatively low pH (about neutral) and a low carbonate concentration shift the chemical equilibrium in favor of $Fe(OH)_2$ precipitation. High Ca^{2+} concentrations in groundwater may compete with Fe^{2+} for carbonate and form $CaCO_3$ minerals as described above.

Precipitation of amorphous ferrous sulfide (FeS) was detected by SEM-EDX in most of the core samples from the Fe^0 barrier (Figure 17). The morphology of FeS appeared to be rounded or bytrodial, and it was commonly observed as coatings on Fe^0 filings or other mineral deposits on iron surfaces. Many Fe^0 particles were completely encrusted in FeS, and these coated Fe^0 filings remained black (rather than rusty) after drying (by vacuum rinsing with acetone), especially those core materials obtained near the interface where groundwater enters the Fe^0 barrier (Phillips et al., 2000). Note that, although there appears to be a high occurrence of FeS, crystalline pyrite was not detected by XRD, perhaps because of the non-crystallinity of the FeS structure. As stated previously, FeS formation in the Fe^0 barrier may be largely attributed to the reduction of SO_4^{2-} to S^{2-} by sulfate-reducing bacteria under a highly reducing

environment in the Fe^0 barrier. Similar observations also have been reported in both laboratory simulated iron columns and field experiments with a relatively high influent sulfate concentration (Gu et al., 1999; Phillips et al., 2000). On the other hand, although reduction of SO_4^{2-} was observed in the Fe^0 barriers at the U.S. Coast Guard Support Center at Elizabeth city, NC, and at an industrial facility in upstate New York (Puls et al., 1999; Vogan et al., 1999), no appreciable amounts of FeS precipitates were observed. These observations may be related to a relatively low SO_4^{2-} concentration (<20 mg/L) present in the groundwaters at these sites.

IV.C. Implications for Long-Term Performance

The occurrence of a suite of mineral precipitates could have serious implications for the long-term performance of Fe^0 reactive barriers. Specifically, these mineral precipitates commonly exist as coating and cementing materials on Fe^0 surfaces. They not only reduce the reactivity of Fe^0 and thus its capacity to degrade or retain target contaminants of concern, but also cause the cementation and clogging of the reactive Fe^0 filings. Ultimately, they may result in reduced hydraulic conductivity or the diversion of groundwater through the barrier. However, site groundwater geochemistry and contaminant concentration may determine the rate and forms of mineral precipitant formation and thus the life span of the Fe^0 permeable reactive barriers. For groundwater of relatively low ionic strength, McMahon *et al.* (1999) estimated a 0.35% yearly loss of total porosity in the iron-reactive media at the Denver Federal Center site. On the other hand, a fast corrosion rate and mineral precipitant formation have been observed at the Oak Ridge Y-12 barrier site, where groundwater contains relatively high concentrations of bicarbonate, sulfate, nitrate, calcium, and magnesium. Isolated spots of clogged and/or cemented

Fe^0 media were observed only ~1.2 years after the installation of the Fe^0 barrier at the Oak Ridge site (Phillips et al., 2000).

Yet more extensive cementation and clogging of iron-reactive media were found in the iron core materials taken ~2.5 years after the installation of the Fe^0 barrier, particularly at the soil/barrier interfaces where groundwater enters the Fe^0 barrier. The cemented iron cores appeared to be hard to break (Figure 18a), and a close examination (by SEM) revealed an extensive iron corrosion and subsequent mineral precipitation on Fe^0 surfaces (Figure 18b). The SEM-EDX analysis of a polished cross-section of the cemented iron filings (Figure 19) indicated that iron oxyhydroxides were the primary mineral precipitates accumulated on or between individual iron particles as a thick rind (Phillips et al., 2000). These iron oxyhydroxides may therefore be largely responsible for the cementation of Fe^0 particles in the barrier. Similarly, Mackenzie *et al.* (1999) reported the portion of an iron column clogged with iron oxyhydroxides to be a hardened solid mass that greatly decreased hydraulic conductivity. Additionally, the precipitation and formation of aragonite and FeS minerals were also at least partially responsible for binding iron particles in cemented iron core samples (Figure 19). In particular, FeS precipitates exist primarily in the form of coatings on iron surfaces and thus may act as active binding agents as well. It is interesting to note the sequence of mineral precipitation on iron surfaces as viewed by SEM of the polished sections (Figure 19). Iron oxyhydroxides appeared to precipitate first as a corrosion product on Fe^0 surfaces. The formation of aragonite followed in response to an increased groundwater pH as a result of iron corrosion, and FeS precipitates then followed as coatings or void fillers on aragonite and iron oxyhydroxide surfaces. The initial delay in the formation of FeS compared with the other precipitates could perhaps be due to the

greater length of time needed for an accumulation of a microbial population to facilitate sulfate reduction in the barrier (Gu et al., 1999; Phillips et al., 2000).

Based on an average Fe^0 filing thickness of ~0.5 to 1.25 mm, Phillips *et al.* (2000) estimated that these Fe^0 filings could be completely corroded within ~5 to <10 years under the specific site geochemical conditions. This estimated life span of an iron reactive barrier is substantially shorter than the life spans that have been estimated previously, ~15 to 30 years (Gillham et al., 1994; Liang et al., 2000; McMahon et al., 1999), and may be explained by the fact that the site groundwater contains relatively high levels of NO_3^- and HCO_3^-, both of which are known to accelerate the corrosion of Fe^0 (Davies and Burstein, 1980; Gu et al., 1999; Huang et al., 1998). It is also important to note that mineral precipitation and iron cementation appeared to occur progressively with time. Within ~1.5 years, spotted cementations of Fe^0 filings were observed mostly at the interface where groundwater enters the Fe^0 barrier. Cementation extended and further developed downgradient of the Fe^0 barrier, as observed in the second coring event (~2.5 years after the barrier was installed). An important implication of these observations is that such an uneven distribution of iron corrosion and mineral precipitation could potentially result in early system clogging at the interface regions and therefore shorten the functional lifetime of in situ Fe^0 barriers. Therefore, close attention should be given to areas in the barrier that seem more vulnerable to corrosion, mineral precipitation, and subsequent cementation (e.g., where groundwater first enters the barriers). Particular attention should also be given to the geochemical composition and concentration in groundwater, which may largely determine the corrosion rate and thus the life span of the Fe^0 reactive barriers.

ACKNOWLEDGMENTS

We thank M. A. Bogle and N. D. Farrow for their technical assistance in field groundwater and core sampling activities, and MSE Technology Applications (W.C. Goldberg) for the first round core sampling. Funding for this research was supported by the Contaminants Focus Area of the Office of Environmental Management (EM-50), U.S. Department of Energy, under contract DE-AC05-00OR22725 with Oak Ridge National Laboratory, which is managed by UT-Battelle, LLC.

REFERENCES

Agrawal, A., and Tratnyek, P. G. (1996). Reduction of nitro aromatic compounds by zero-valent iron metal. *Environ. Sci. Technol.* **30**, 153-160.

Agrawal, A., Tratnyek, P. G., Stoffyn-Egli, P., and Liang, L. (1995). Processes affecting nitro reduction by iron metal: Mineralogical consequences of precipitation in aqueous carbonate environments. *209th ACS National Meetings, American Chemical Society* **35**, 720-723.

Baes, C. F., and Mesmer, R. E. (1976). "The hydrolysis of cations," John Wiley & Sons, New York.

Blowes, D. W., Ptacek, C. J., and Jambor, J. L. (1997). In-situ remediation of Cr(VI)-contaminated gruondwater using permeable reactive walls: laboratory studies. *Environ. Sci. Technol.* **31**, 3348-3357.

Cantrell, K. J., Kaplan, D. I., and Wietsma, T. W. (1995). Zero-valent iron for the in situ remediation of selected metals in groundwater. *J. Haz. Mater.* **42**, 201-212.

Chee-Sanford, J. C., Frost, J. W., Fries, M. R., Zhou, J., and Tiedje, J. M. (1996). Evidence for acetyl coenzyme A and cinnamoyl coenzyme A in the anaerobic toluene mineralization pathway in Azoarcus tolulyticus Tol-4. *Applied Environ. Microbiol.* **62**, 964-973.

Cook, P. G., Solomon, D. K., Sanford, W. E., Busenberg, E., Plummer, L. N., and Poreda, R. J. (1996). Inferring shallow groundwater flow in saprolite and fractured rock using environmental tracers. *Wat. Res.* **32**, 1501-1509.

Davies, D. H., and Burstein, G. T. (1980). The effects of bicarbonate on the corrosion and passivation of iron. *Corr.* **36**, 416-422.

Dowling, J. E., Widdel, F., and White, D. C. (1986). Phospholipid ester-linked fatty acid biomarkers of acetate-oxidizing sulfate reducers and other sulfide-forming bacteria. *J. Gen. Microbiol.* **132**, 1815-1825.

Edwards, R. W., Duster, D., Faile, M., Gallant, W., Gibeau, E., Myller, B., Nevling, K., and O'Brady, B. (1996). *RTDF Permeable reactive barriers action team meeting,* August 15-16. San Francisco, CA.

Fiedor, J. N., Bostick, W. D., Jarabek, R. J., and Farrell, J. (1998). Understanding the mechanism of uranium removal from gruondwater by zero-valent iron using X-ray photoelectron spectroscopy. *Environ. Sci. Technol.* **32**, 1466-1473.

Gillham, R. W., Blowes, D. W., Ptacek, C. J., and O'Hannesin, S. F. (1994). Use zero-valent metals in in-situ remediation of contaminated groundwater. In "*In-Situ remediation: scientific basis for current and future technologies*" (G. W. Gee and N. R. Wing, eds.), Battelle Press, Columbus, Richland. pp. 913-929.

Gu, B., Liang, L., Dickey, M. J., Yin, X., and Dai, S. (1998). Reductive precipitation of uranium(VI) by zero-valence iron. *Environ. Sci. Technol.* **32**, 3366-3373.

Gu, B., Liang, L., Dickey, M. J., Yin, X., and Watson, D. (1997). In Situ reactive barriers for simulteneous treatment of radionuclides and chlorinated organic contaminants. *RTDF Permeable reactive barriers action team meeting,* Virginia Beach, VA. September 18-19, pp 46-47.

Gu, B., Phelps, T. J., Liang, L., Dickey, M. J., Roh, Y., Kinsall, B. L., Palumbo, A. V., and Jacobs, G. K. (1999). Biogeochemical dynamics in zero-valent iron columns: implications for permeable reactive barriers. *Environ. Sci. Technol.* **33**, 2170-2177.

Gu, B., Zhou, J. Z., Watson, D. B., Phillips, D. H., and Wu, L. (2001). Microbiological characteristics in a zero-valent iron reactive barrier. *Environ. Monit. Ass.*, (in Review).

Guckert, J. B., Hood, M. A., and White, D. C. (1986). Phospholipid, ester-linked fatty acid profile changes during nutrient deprivation of *Vibrio Cholerae*: increases in the *trans/cis* ratio and productions of cyclopropyl fatty acids. *Appl. Environ. Microbiol.* **52**, 794-801.

Gui, J., and Devine, T. M. (1994). The influence of sulfate ions on the surface enhanced Raman spectra of passive films formed on iron. *Corr. Sci.* **36**, 441-462.

Horwitz, E. P., Dietz, M. L., Chiarizia, R., and Diamond, H. (1992). Separation and preconcentration of uranium from acidic media by extraction chromatography. *Anal. Chim. Acta* **266**, 25-37.

Hsi, C. K. D., and Langmuir, D. (1985). Adsorption of uranyl onto ferric oxyhydroxides: application of the surface complexation site-binding model. *Geochim. Cosmochim. Acta* **49**, 1931-1941.

Huang, C. P., Wang, H. W., and Chiu, P. C. (1998). Nitrate reduction by metallic iron. *Water Res.* **32**, 2257-2262.

Johnson, T. L., and Tratnyek, P. G. (1994). A column study of geochemical factors affecting reductive dechlorination of chlorinated solvents by zero-valent iron. In "*In-Situ Remediation: Scientific Basis for Current and Future Technologies*" (G. W. Gee and N. R. Wing, eds.), Vol. 2, Battelle Pacific Northwest Laboratories. Pasco, WA. pp. 931-947.

Liang, L., Korte, N., Goodlaxson, J. D., Clausen, J., Fernando, Q., and Muftikian, R. (1997). Byproduct formation during the reduction of TCE by zero-valence iron and palladized iron. *GWMR, Winter*, 122-127.

Liang, L., Korte, N., Gu, B., Puls, R., and Reeter, C. (2000). Geochemical and microbiological reactions affecting the long-term performance of in situ iron barriers. *Adv. Environ. Res.* **4**, 273-286.

Lipczynska-Kochany, E., Harms, S., and Nadarajah, N. (1994). Degradation of carbon tetrachloride in the presence of iron and sulphur containing compounds. *Chemosphere* **29**, 1477-1489.

Mackenzie, P. D., Horney, D. P., and Sivavec, T. M. (1999). Mineral precipitation and porosity losses in granular iron columns. *J. Haz. Mat.* **68**, 1-17.

Mackenzie, P. D., Sivavec, T. M., and Horney, D. P. (1997). Extending hydraulic lifetime of iron walls. *International Containment Technology Conference and Exhibition,* St. Petersburg, FL., pp 781-786.

McMahon, P. B., Dennehy, K. F., and Sandstrom, M. W. (1999). Hydraulic and geochemical performance of a permeable reactive barrier containing zero-valent iron, Denver Federal Center. *Ground Water* **37**, 396-404.

Morrison, S. J., Spangler, R. R., and Tripathi, V. S. (1995). Adsorption fo uranium (VI) on amorphous ferric oxyhydroxide at high concentrations of dissolved carbon(IV) and sulfur(VI). *J. Contaminant Hydrol.* **17**, 333.

Morse, J. W., and Choppin, G. R. (1991). The chemistry of transuranic elements In natural waters. *Rev. Aquatic Sci.* **4**, 1-22.

Odziemkowski, M. S., Schumacher, T. T., and Reardon, E. J. (1998). Mechanism of oxide film formation on iron in simulating groundwater solutions: Raman spectroscopic studies. *Corr. Sci.* **40**, 371-389.

O'Hannesin, S. F., and Gillham, R. W. (1998). Long-term performance of an in situ "Iron Wall" for remediation of VOCs. *Groundwater* **36**, 164-172.

Phillips, D. H., Gu, B., Watson, D. B., and Roh, Y. (2001). Impact of sample preparation on mineralogical analysis of iron reactive barrier materials. *Environ. Sci. Technol.*, (in review).

Phillips, D. H., Gu, B., Watson, D. B., Roh, Y., Liang, L., and Lee, S. Y. (2000). Performance evaluation of a zero-valent iron reactive barrier: mineralogical characteristics. *Environ. Sci. Technol.* **34**, 4169-4176.

Pratt, A. R., Blowes, D. W., and Ptacek, C. J. (1997). Products of chromate reduction on proposed subsurface remediation material. *Environ. Sci. Technol.* **31**, 2492-2498.

Puls, R. W., Paul, C. J., and Powell, R. M. (1999). The application of in situ permeable reactive (zero-valent iron) barrier technology for the remediation of chromate-contaminated groundwater: a field test. *Appl. Geochem.* **14**, 989-1000.

Roberts, A. L., Totten, L. A., A., A. W., Burris, D. R., and Campbell, T. J. (1996). Reductive elimination of chlorinated ethylenes by zero-valent metals. *Environ. Sci. Technol.* **30**, 2654-2659.

Roh, Y., Lee, S. Y., and Elless, M. P. (2000). Characterization of corrosion products in the permeable reactive barriers. *Environ. Geol.* **40**, 184-194.

SAIC (1996). Bear Creek Valley characterization area technology demonstration action plan. *SY/EN-5479.* Science Applications International Corporation, Oak Ridge, TN 37831.

SAIC (1997). Phase I report on the Bear Creek Valley Treatability study, Oak Ridge Y-12 Plant, Oak Ridge, Tennessee. *Y/ER-285.* Science Applications International Corporation, Oak Ridge, TN 37831.

Scherer, M. M., Balko, B. A., and Tratnyek, P. G. (1998). The role of oxides in reduction reactions at the metal-water interface. In "*Kinetics and mechanisms of reactions at the mineral-water interface*" (D. Sparks and T. Grundl, eds.). American Chemical Society: Washington, DC.

Scherer, M. M., Richter, S., Valentine, R. L., and Alvarez, P. J. (2000). Chemistry and microbiology of permeable reactive barriers for in situ groundwaer cleanup. *Crit. Rev. Environ. Sci. Technol.* **30**, 363-411.

Schwertmann, U., and Cornell, R. M. (1991). "Iron oxide in the laboratory: preparation and characterization," VCH Pub., New York.

Schwertmann, U., and Taylor, R. M. (1977). In "*Minerals in Soil Environments*" (J. Dixon and S. B. Weed, eds.), Soil Sci. Soc. Amer. pp. 145-180.

Shoemaker, S. H., Greiner, J. F., and Gillham, R. W. (1995). Permeable reactive barriers. In "*Assessment of barrier containment technologies*" (R. R. Rumer and J. K. Mitchell, eds.), Section 11, pp 301-353.

Sivavec, T. M., Mackenzie, P. D., Horney, D. P., and Baghel, S. S. (1997). Redox-active media for permeable reactive barriers. *2nd International Containment Technology Conference,* St. Petersburg, FL., pp 753-759.

Tratnyek, P. G., Johnson, T. L., Scherer, M. M., and Eykholt, G. R. (1997). Remediating ground water with zero-valent metals: chemical considerations in barrier design. *GWMR* **17**, 108-114.

Tunlid, A., and White, D. C. (1991). Biochemical analysis of biomass, community structure, nutritional status and metabolic activity of the microbial communities in soil. In "*Soil Biochemistry, Vol. 7*" (J. M. Bollag and G. Stotzky, eds.), New York. pp. 229-262.

Vogan, J. L., Focht, R. M., Clark, D. K., and Graham, S. L. (1999). Performance evaluation of a permeable reactive barrier for remediation of dissolved chlorinated solvents in groundwater. *J. Haz. Mat.* **68**, 97-108.

Watson, D., Gu, B., Phillips, D. H., and Lee, S. Y. (1999). Evaluation of permeable reactive barriers for removal of uranium and other inorganics at the Department of Energy Y-12 Plant, S-3 disposal ponds. *ORNL/TM-1999/143*, Oak Ridge National Laboratory, Oak Ridge, TN.

Zhou, J. Z., Bruns, M. A., and Tiedje, J. M. (1996). DNA recovery from soils of diverse composition. *Appl. Environ. Microbiol.* **62**, 461-468.

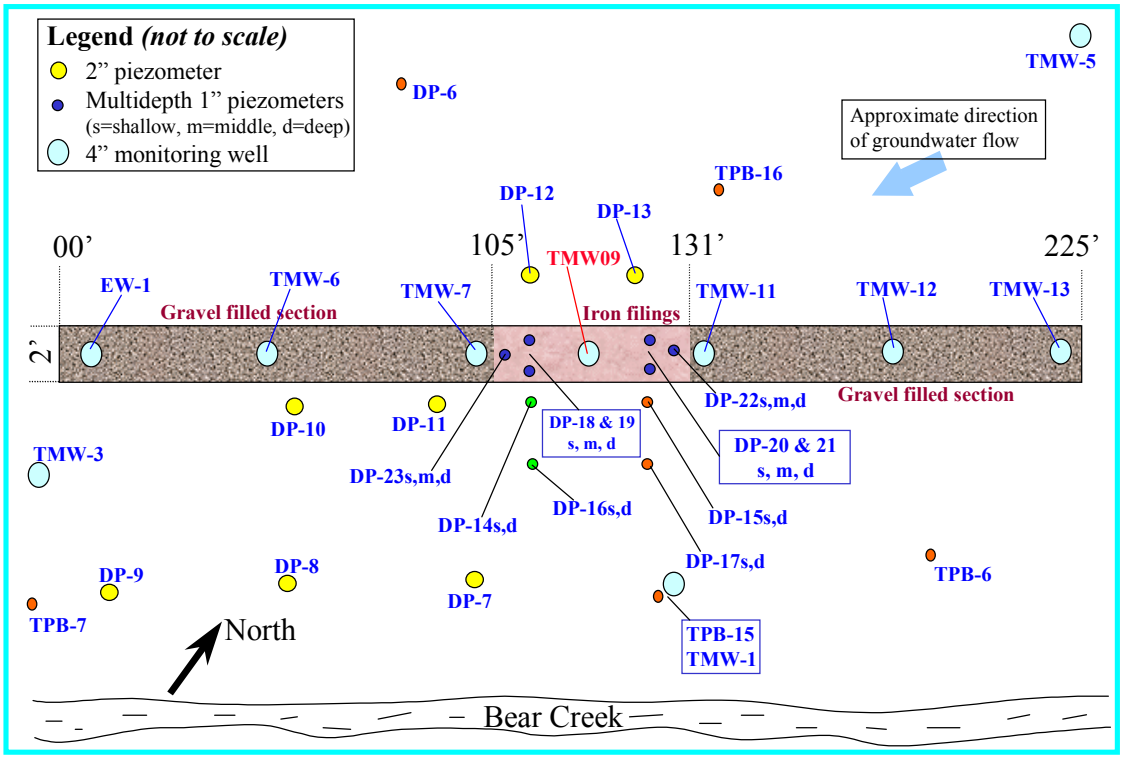

Figure 1. "Aerial view" of the permeable iron-gravel trench barrier and location of monitoring wells and piezometers at the Y-12 site, Oak Ridge, Tennessee. The trench dimensions are approximately 225 ft long, 30 ft deep, and 2 ft wide with the Fe^0-filled mid-section of ~26 ft.

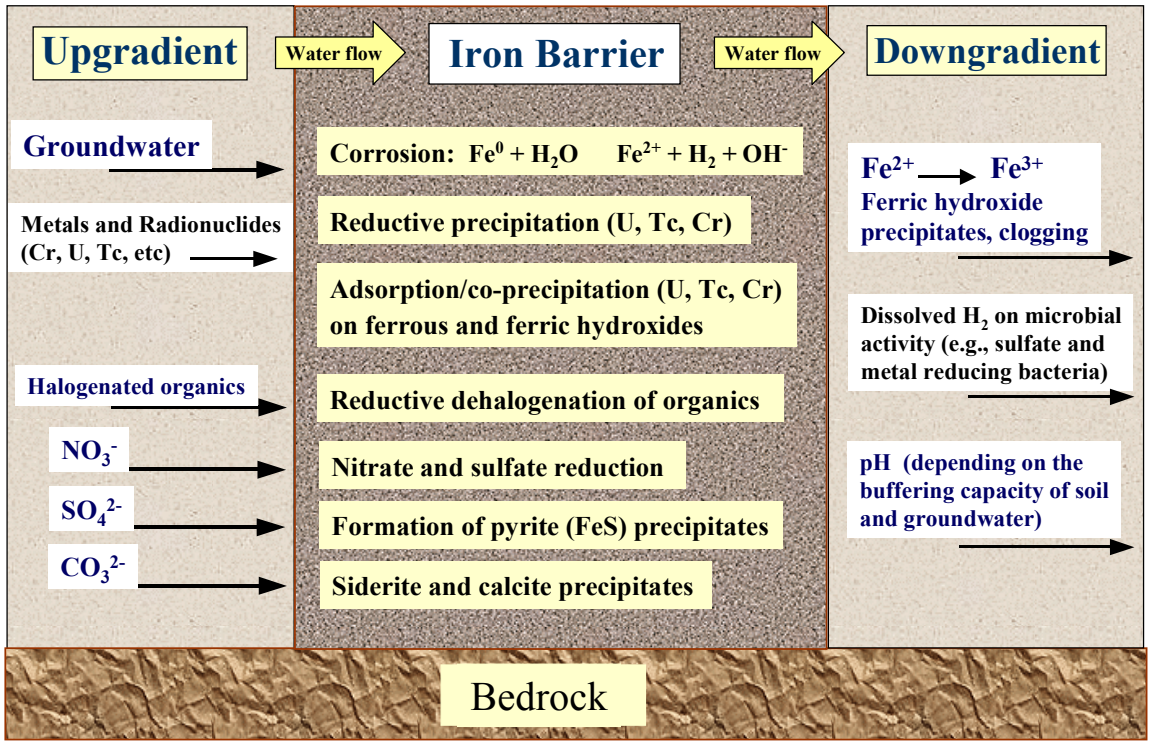

Figure 2. Examples of possible biogeochemical reactions occurring within and in the vicinity of the iron reactive barrier.

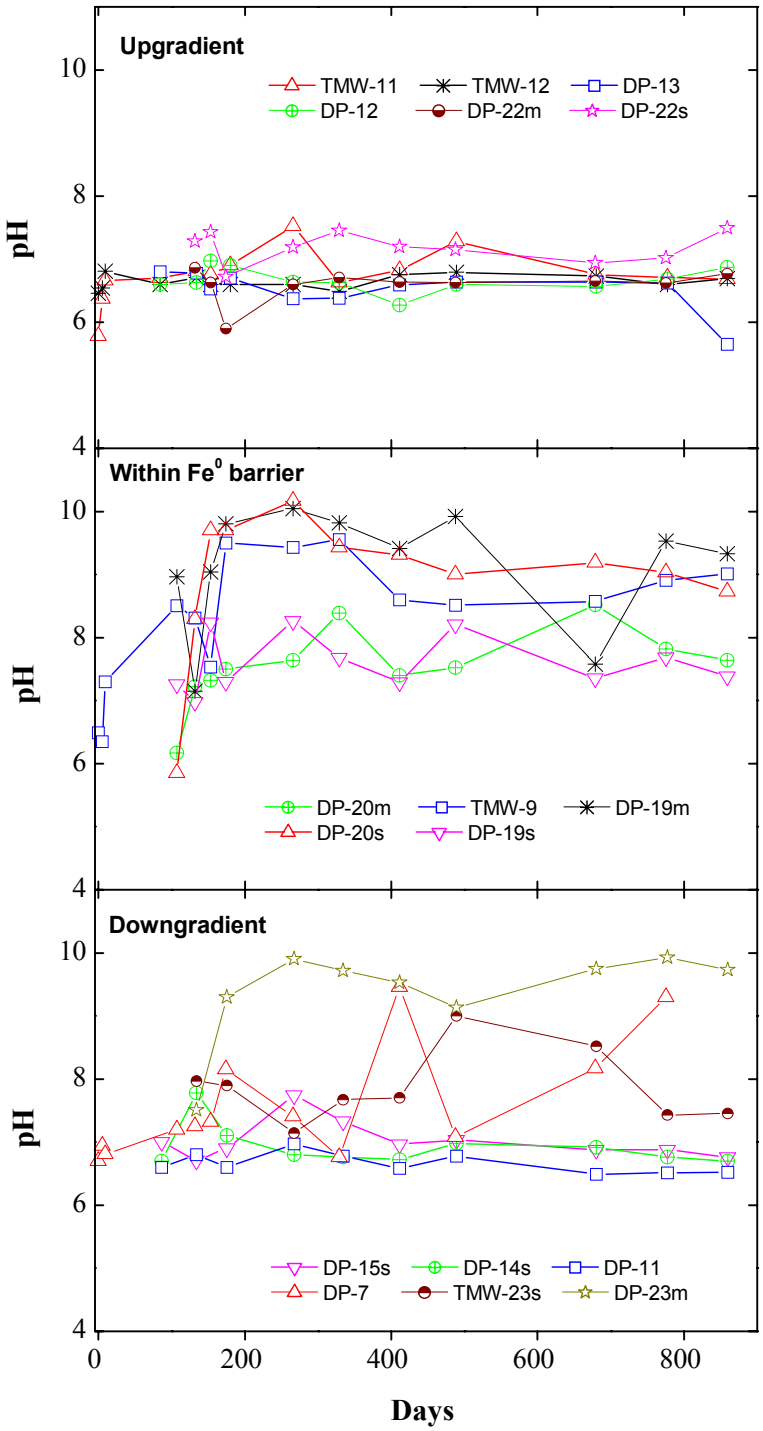

Figure 3. Groundwater pH in some selected monitoring wells within and in the vicinity of the Fe^0 reactive barrier at the Y-12 site, Oak Ridge, Tennessee. The barrier was installed on November 30, 1997 (Time = 0).

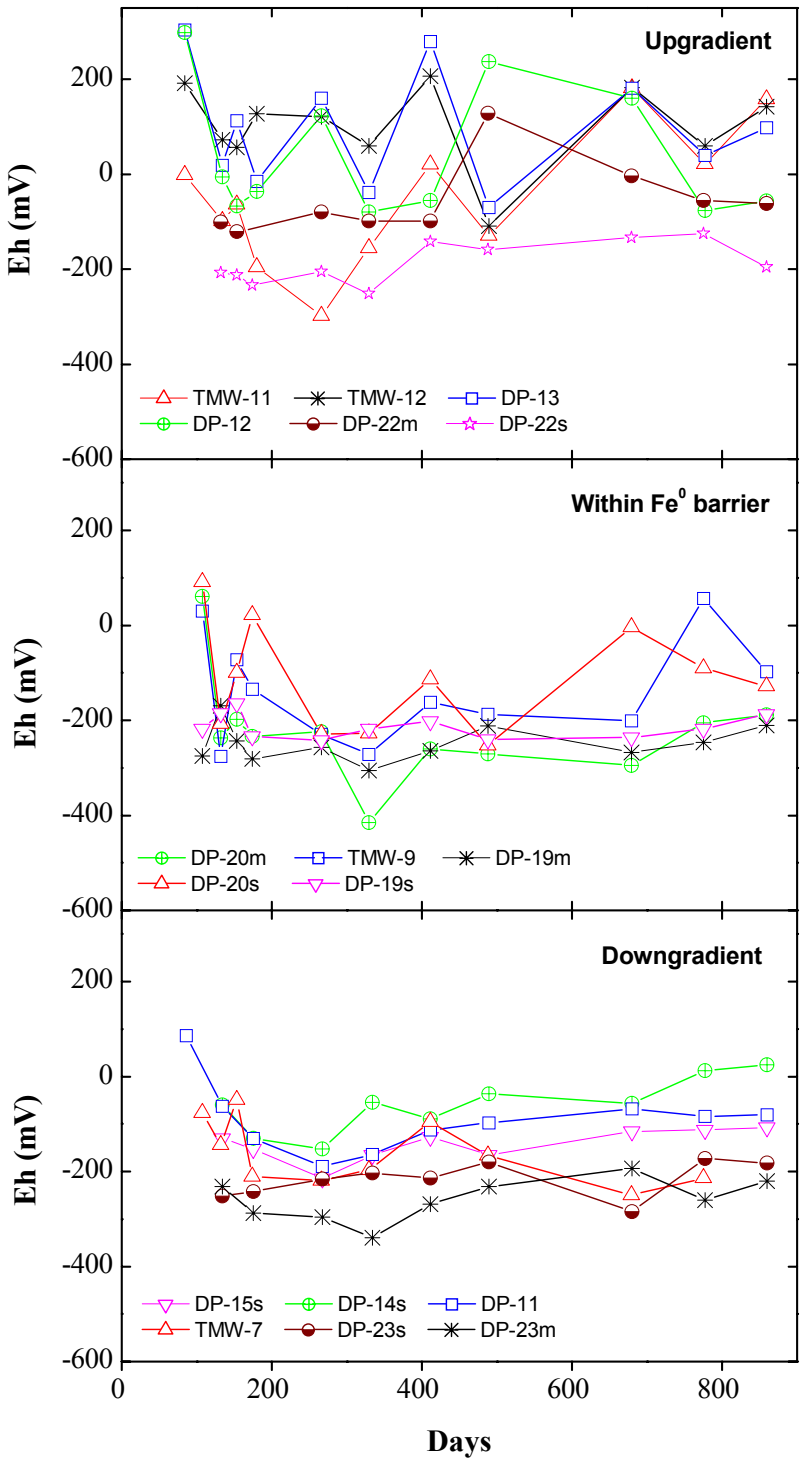

Figure 4. Groundwater redox potential (Eh) in some selected monitoring wells within and in the vicinity of the Fe^0 reactive barrier at the Y-12 site, Oak Ridge, Tennessee.

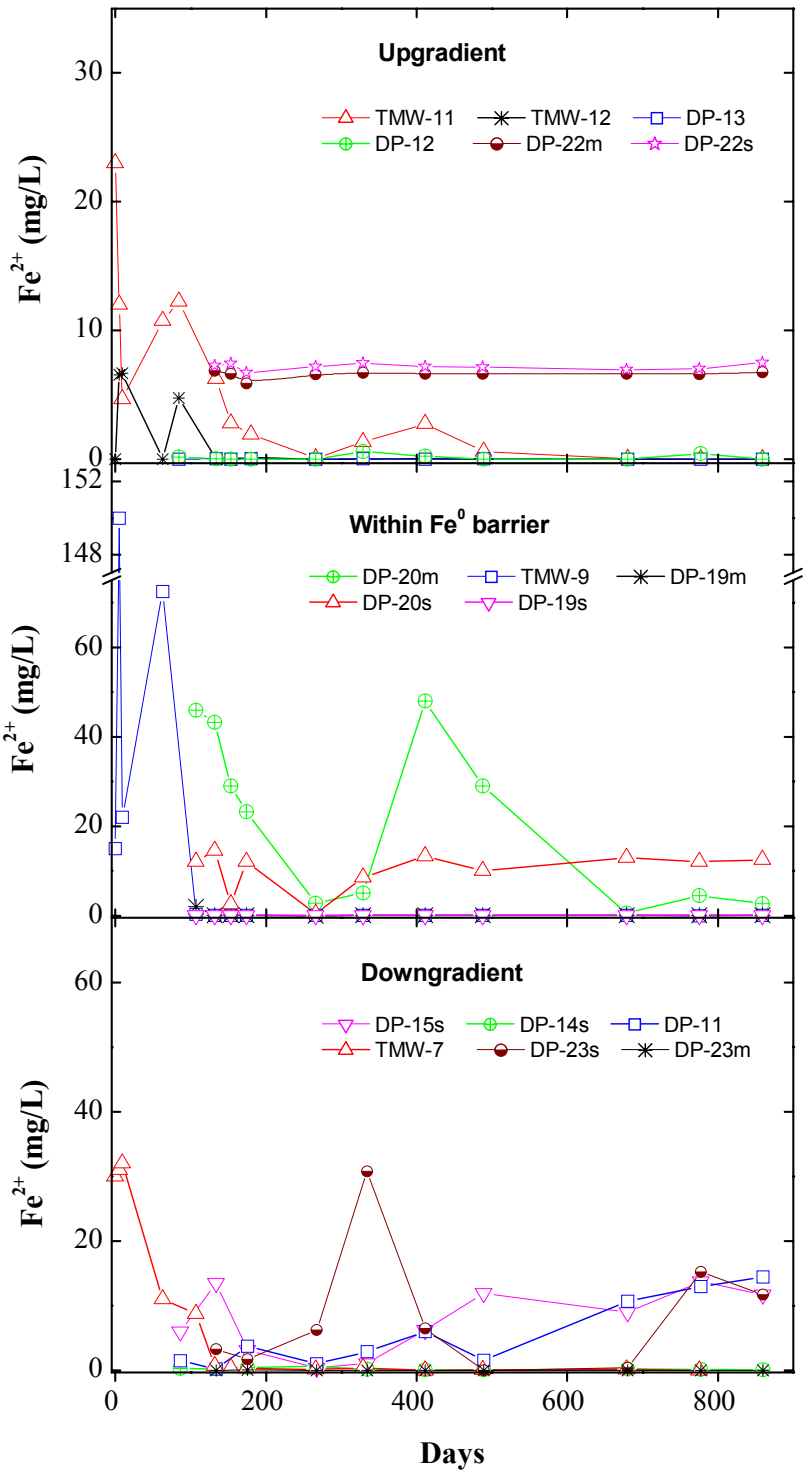

Figure 5. Ferrous (Fe^{2+}) concentration in some selected monitoring wells within and in the vicinity of the Fe^0 reactive barrier at the Y-12 site, Oak Ridge, Tennessee.

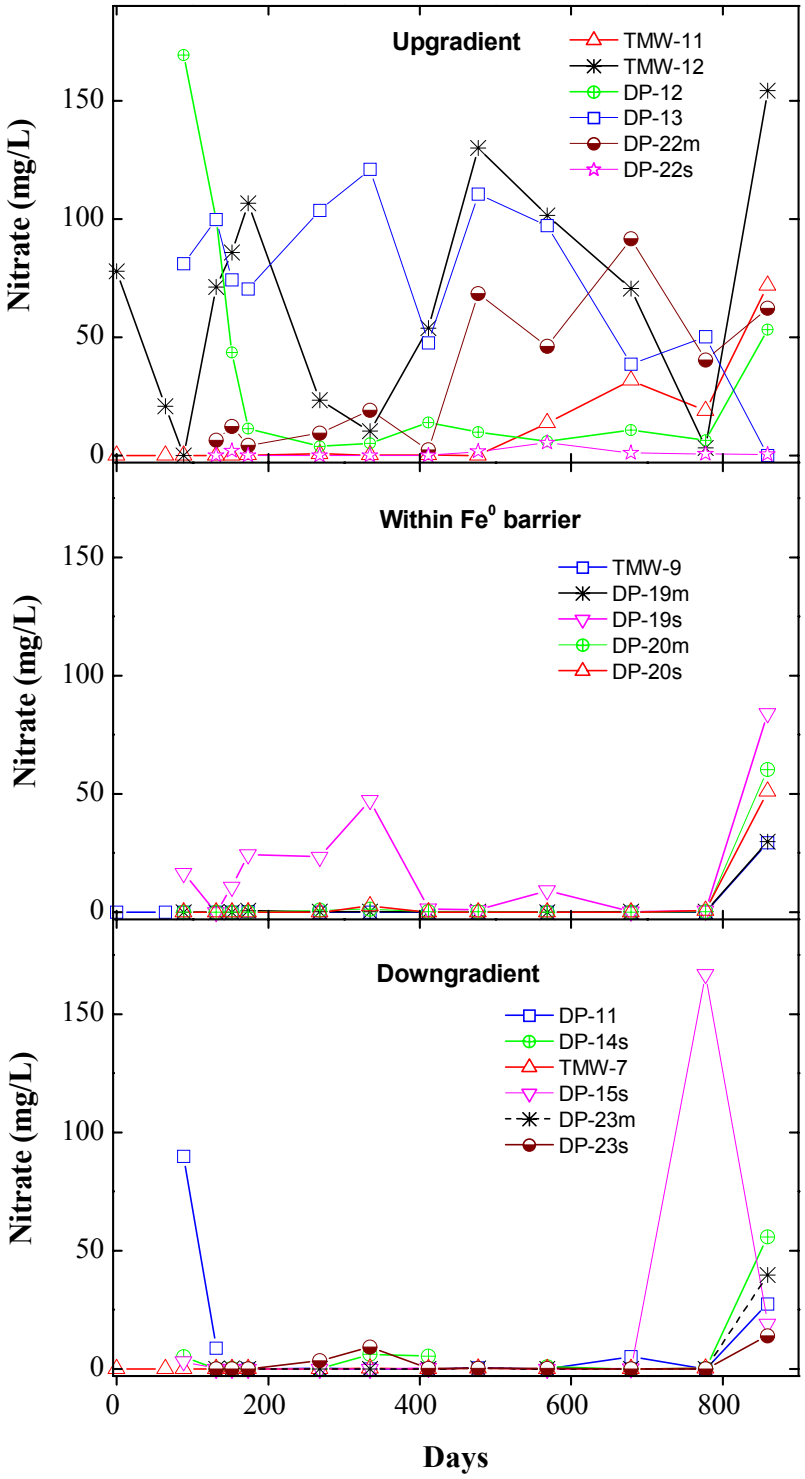

Figure 6. Nitrate concentration profiles in some selected monitoring wells within and in the vicinity of the Fe^0 reactive barrier at the Y-12 site, Oak Ridge, Tennessee.

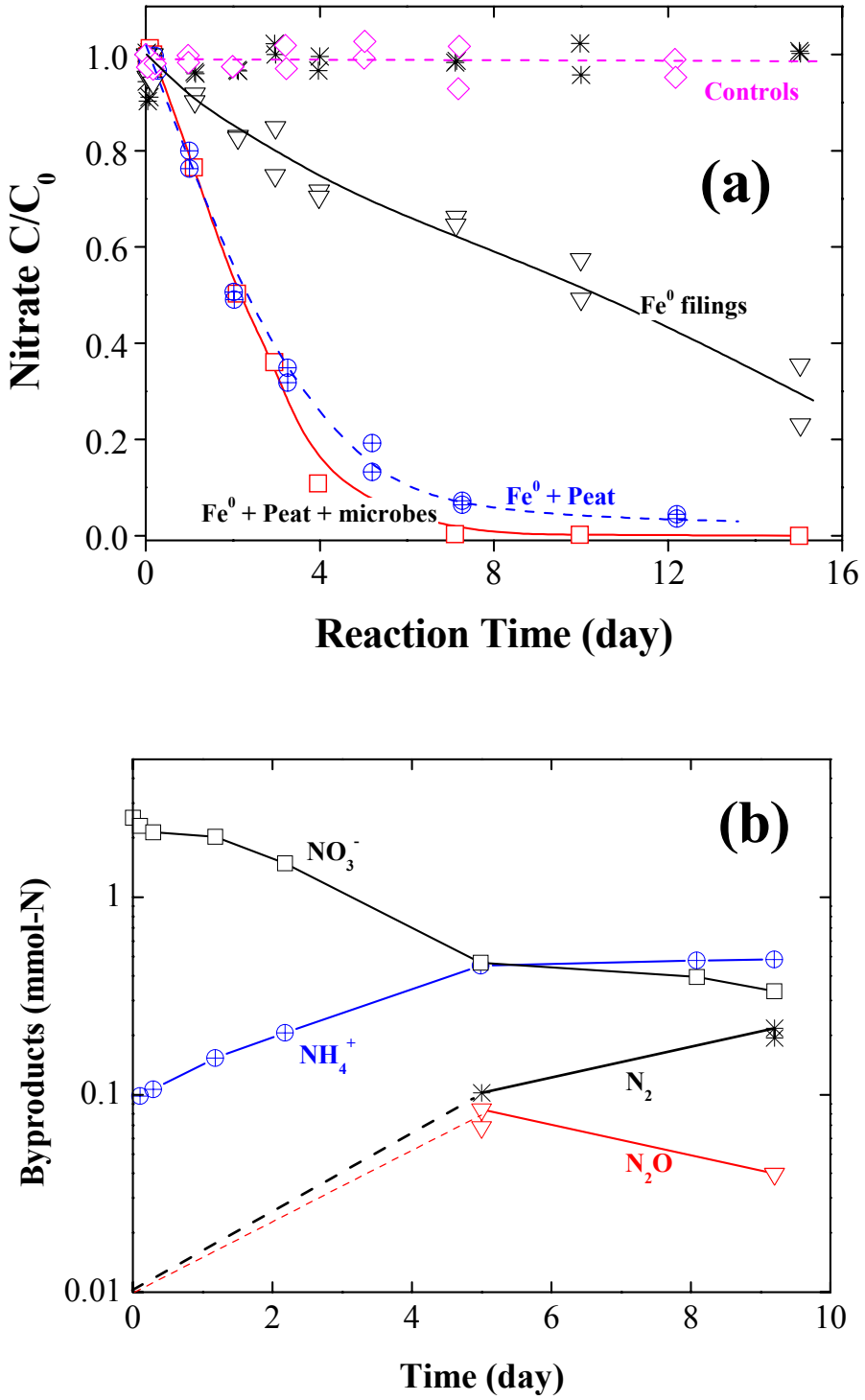

Figure 7. (a) Nitrate degradation kinetics with Fe^0 filings, or a mixture of Fe^0 filings with Wards peat and/or an *Azoarcus tolulyticus* Tol-4 denitrifying bacterium. Initial NO_3^- concentration was 6,000 mg/L in these laboratory studies, and controls were added with Wards peat or Tol-4 bacterium only (without addition of Fe^0 filings). (b) Identification of NO_3^- degradation byproducts with Fe^0 filings and Wards peat.

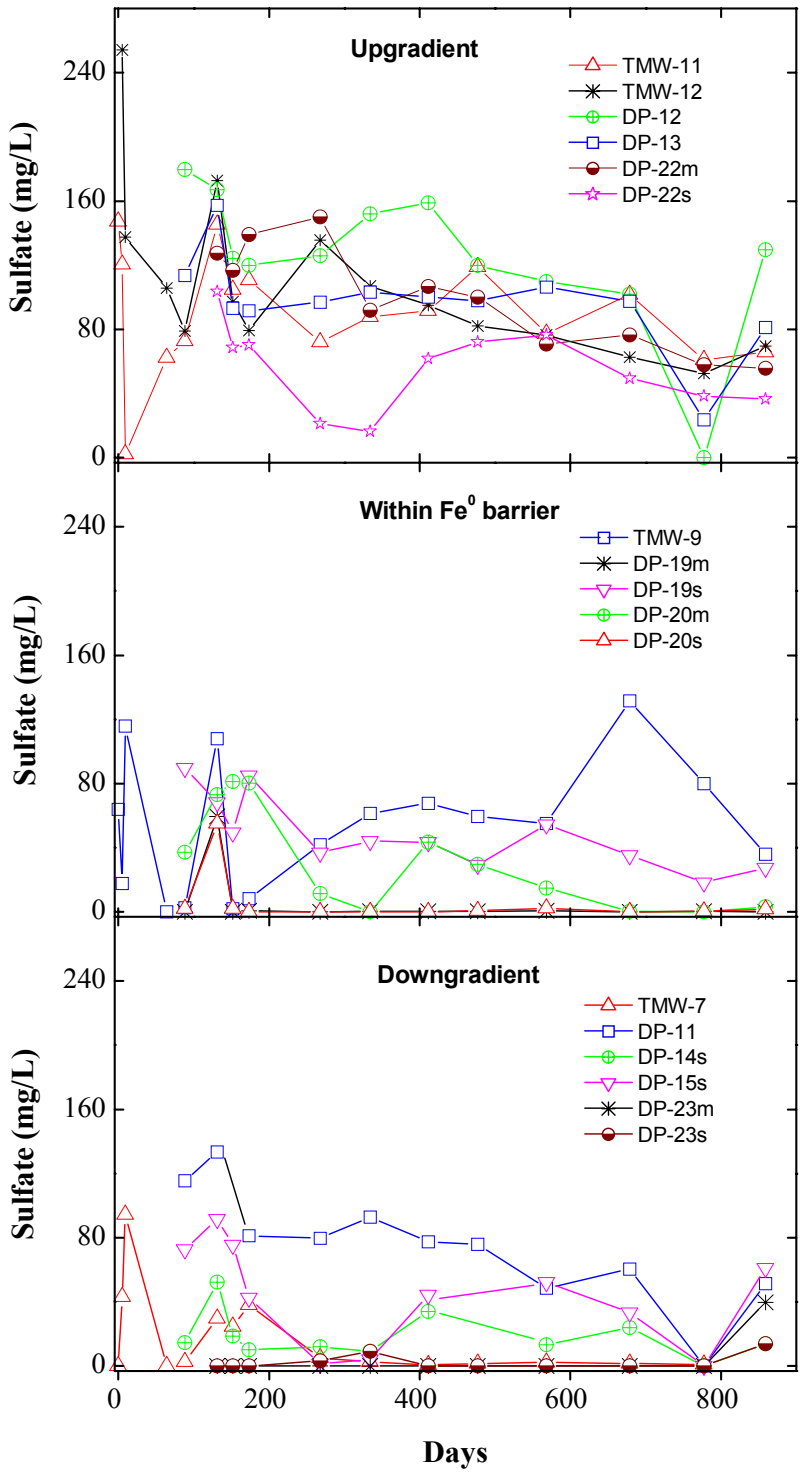

Figure 8. Sulfate concentration profiles in some selected monitoring wells within and in the vicinity of the Fe^0 reactive barrier at the Y-12 site, Oak Ridge, Tennessee.

Figure 9. Uranium concentration profiles in some selected monitoring wells within and in the vicinity of the Fe^0 reactive barrier at the Y-12 site, Oak Ridge, Tennessee.

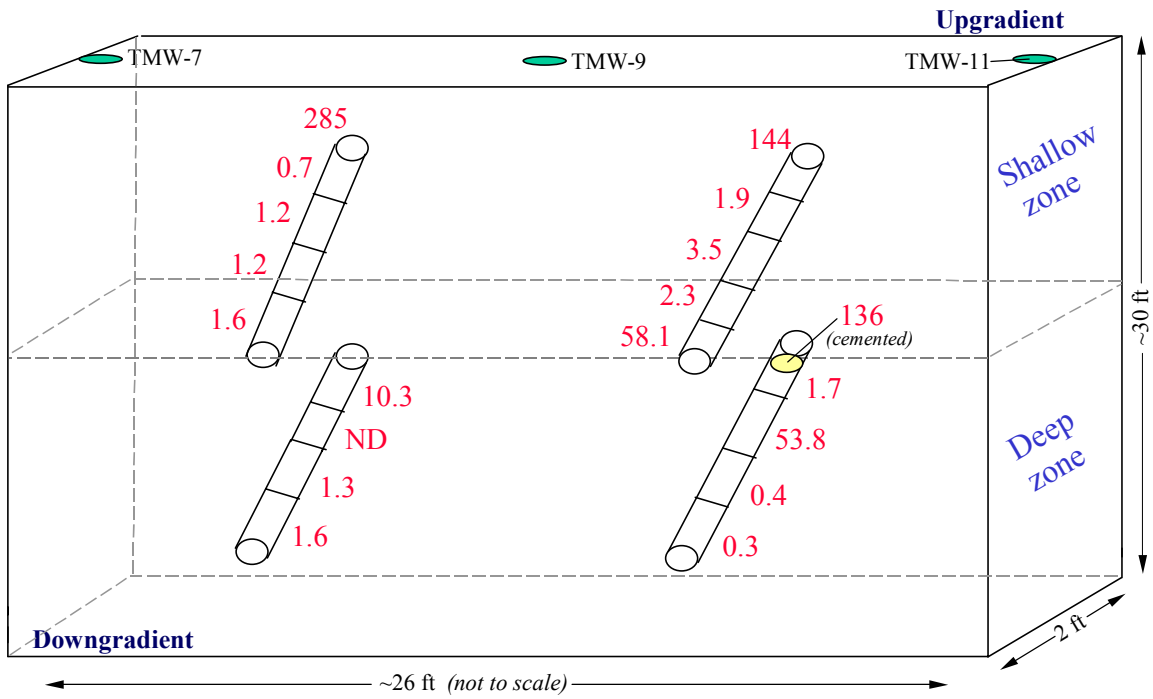

Figure 10. Distribution of uranium (mg/kg) in core samples within the Fe^0 portion of the iron/gravel trench barrier. Angled core samples (60 degree) were collected from upgradient to downgradient of the Fe^0 barrier in February 1999 (Phillips *et al.* 2000).

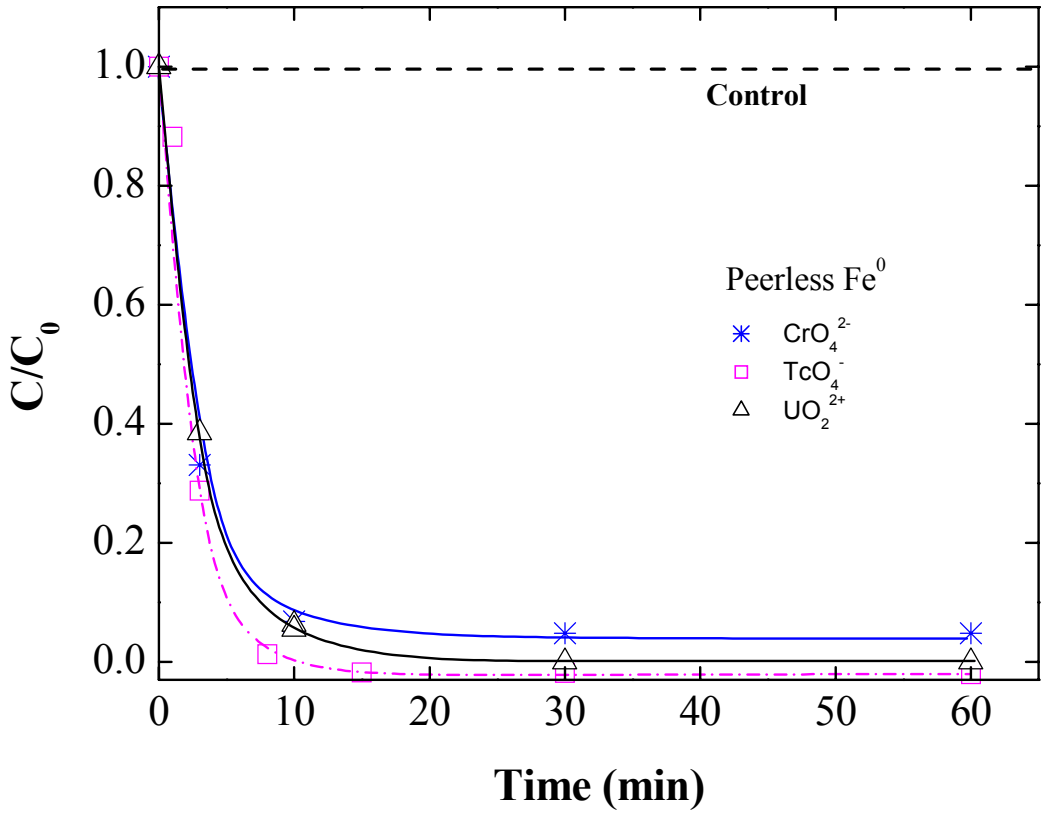

Figure 11. Reaction kinetics of contaminant metals (UO_2^{2+}, CrO_4^{2-}, and TcO_4^-) by Peerless Fe^0 filings in water. Initial concentrations (C_0) were 1000 mg U/L, 10 mg Cr/L, and 6 µg Tc/L, respectively.

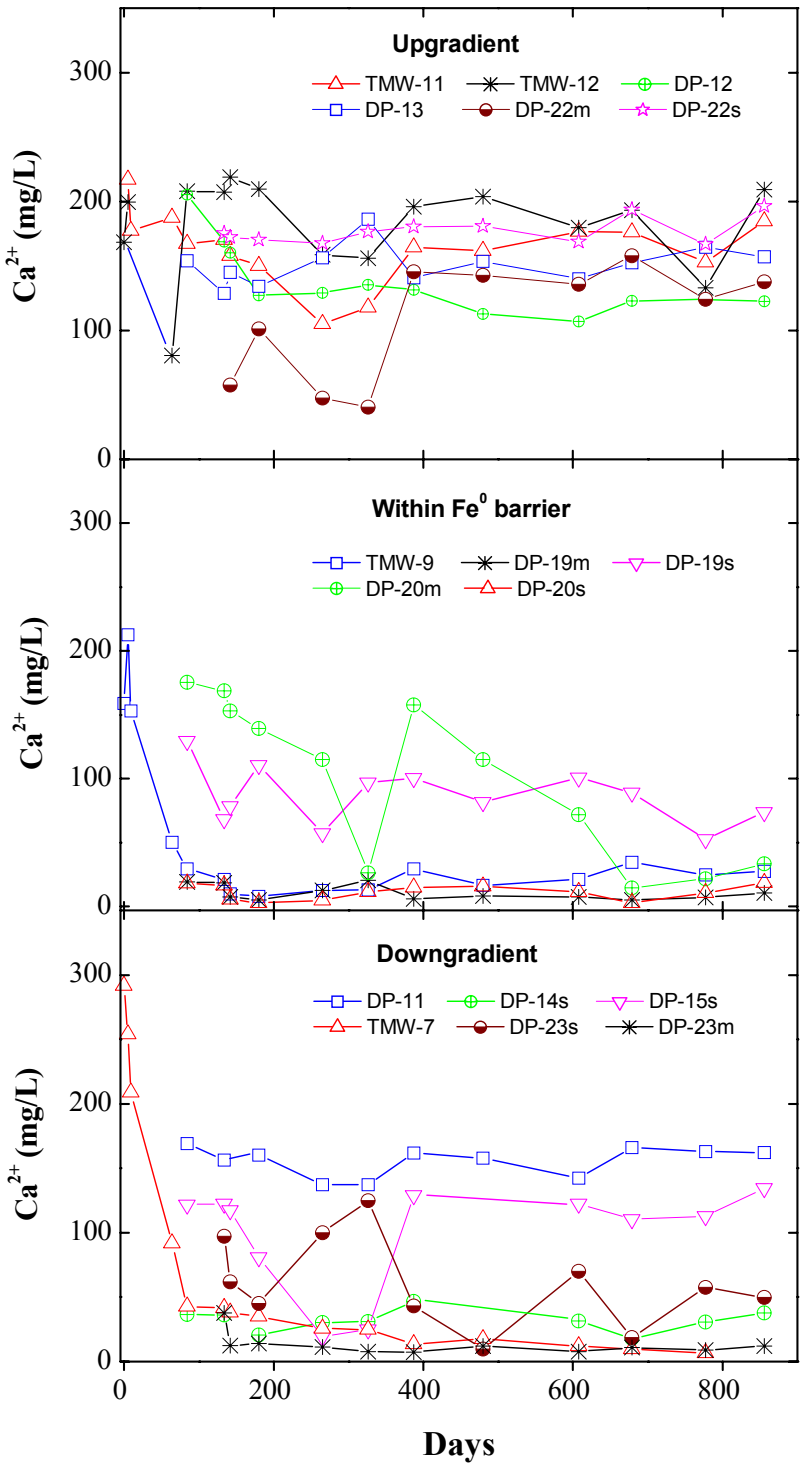

Figure 12. Calcium concentration profiles in some selected monitoring wells within and in the vicinity of the Fe^0 reactive barrier at the Y-12 site, Oak Ridge, Tennessee.

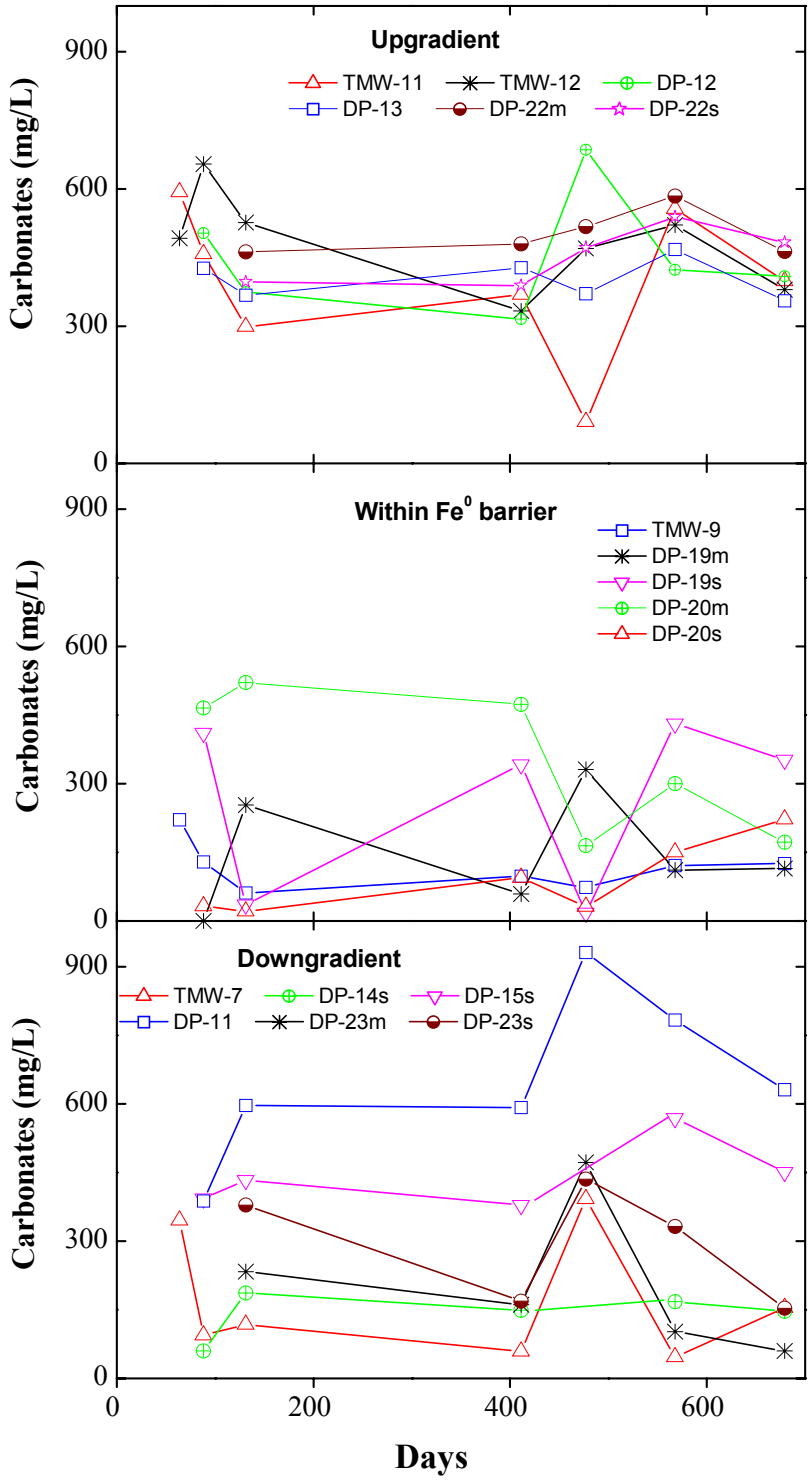

Figure 13. Carbonate/bicarbonate concentration profiles in some selected monitoring wells within and in the vicinity of the Fe^0 reactive barrier at the Y-12 site, Oak Ridge, Tennessee.

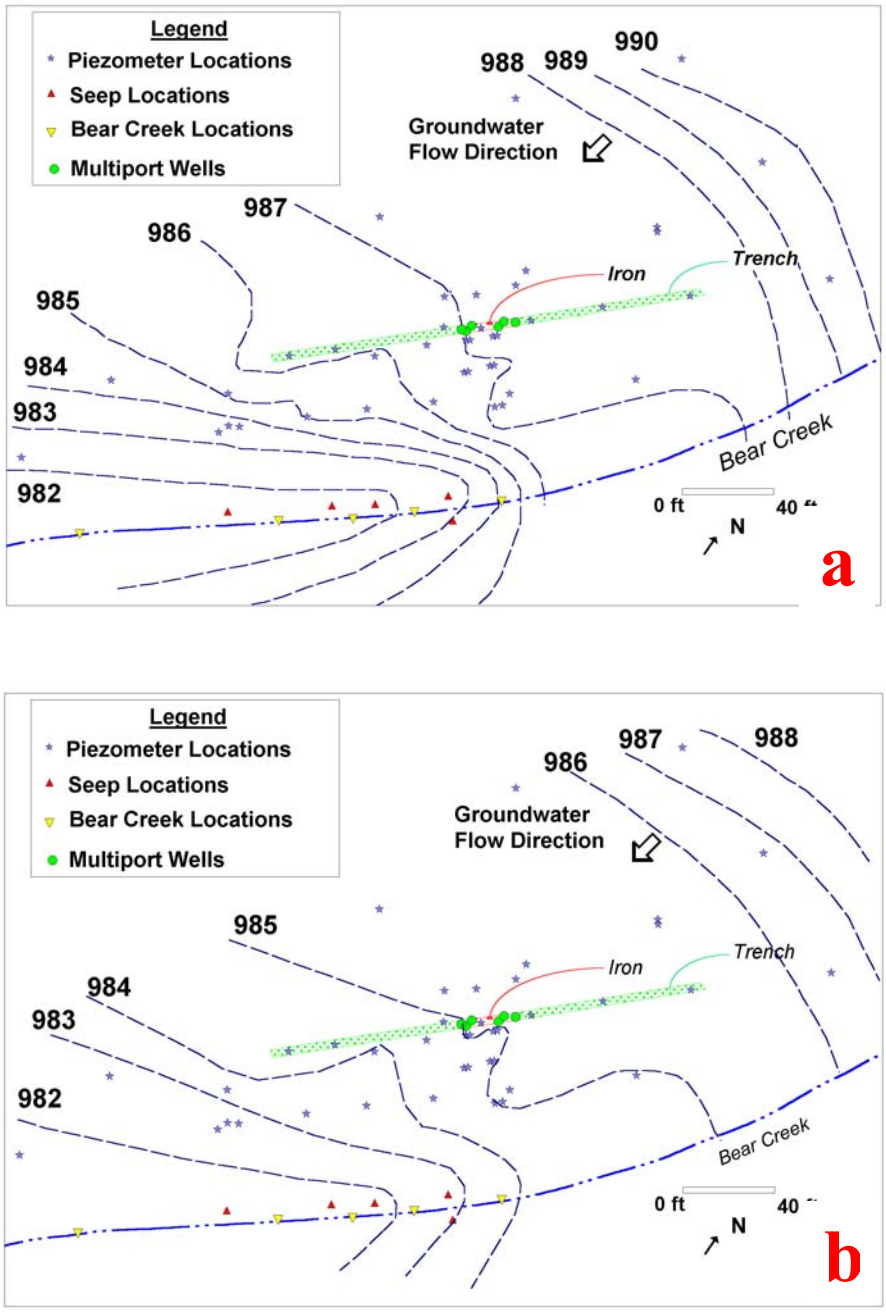

Figure 14. Comparison of groundwater levels (ft) measured on May 6, 1998 (a) and May 17, 2000 (b) at the Y-12 reactive barrier site, Oak Ridge, Tennessee.

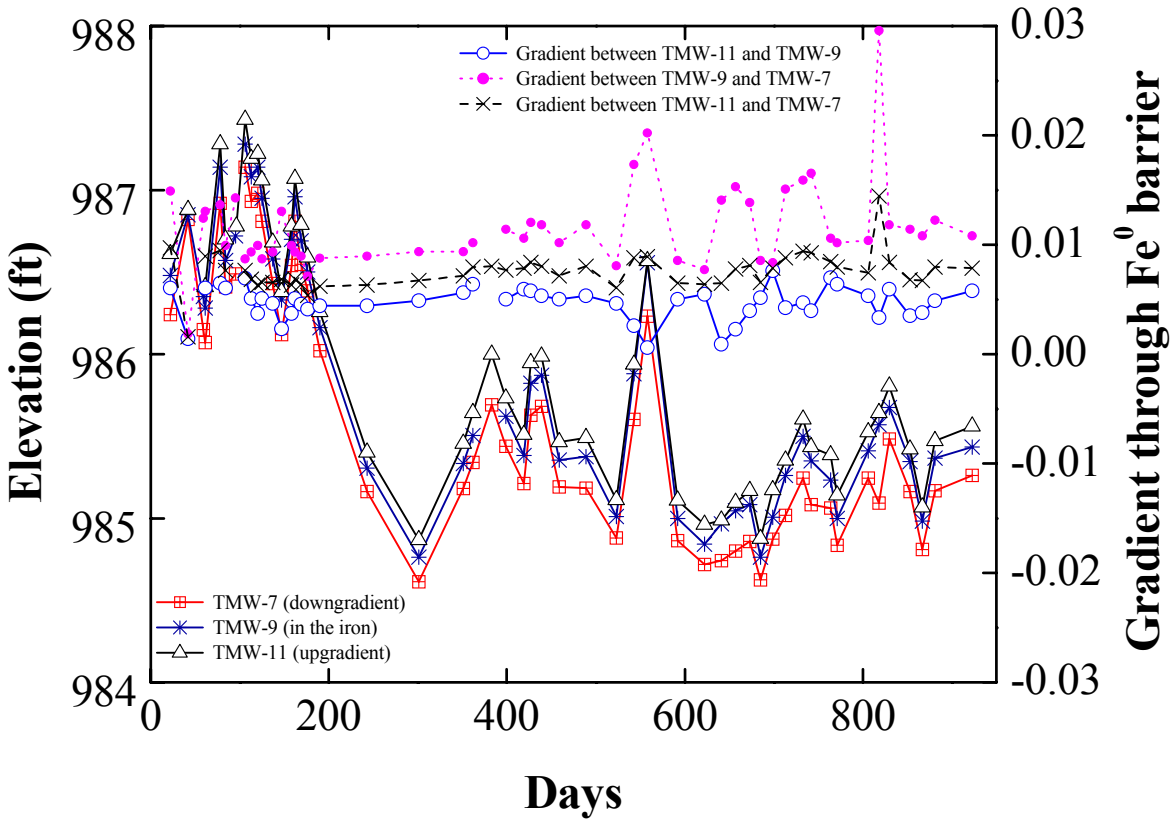

Figure 15. Groundwater elevations and gradients (ft) in some selected monitoring wells upgradient or downgradient of the iron reactive barrier at the Y-12 site, Oak Ridge, Tennessee.

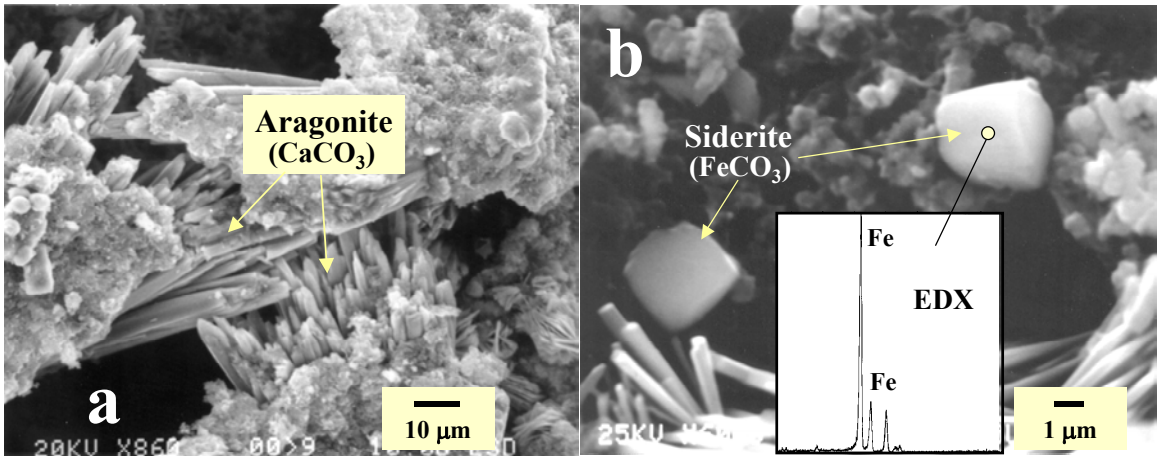

Figure 16. Carbonate minerals in the Fe^0 barrier: (a) characteristic aragonite ($CaCO_3$) crystals and (b) cubed shaped siderite ($FeCO_3$) and its composition identified by energy dispersive x-ray (EDX) analysis.

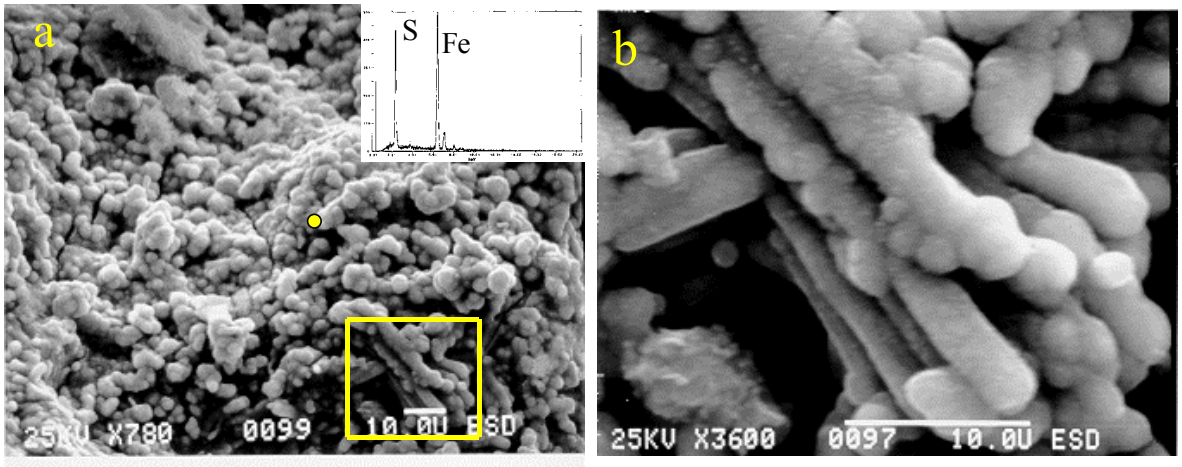

Figure 17. Photomicrographs of amorphous FeS in the Fe^0 barrier: (a) the rounded or bytrodial amorphous FeS coating materials in a cemented zone of the Fe^0 barrier and (b) enlargement of an area of (a) showing FeS coatings on aragonite crystals.

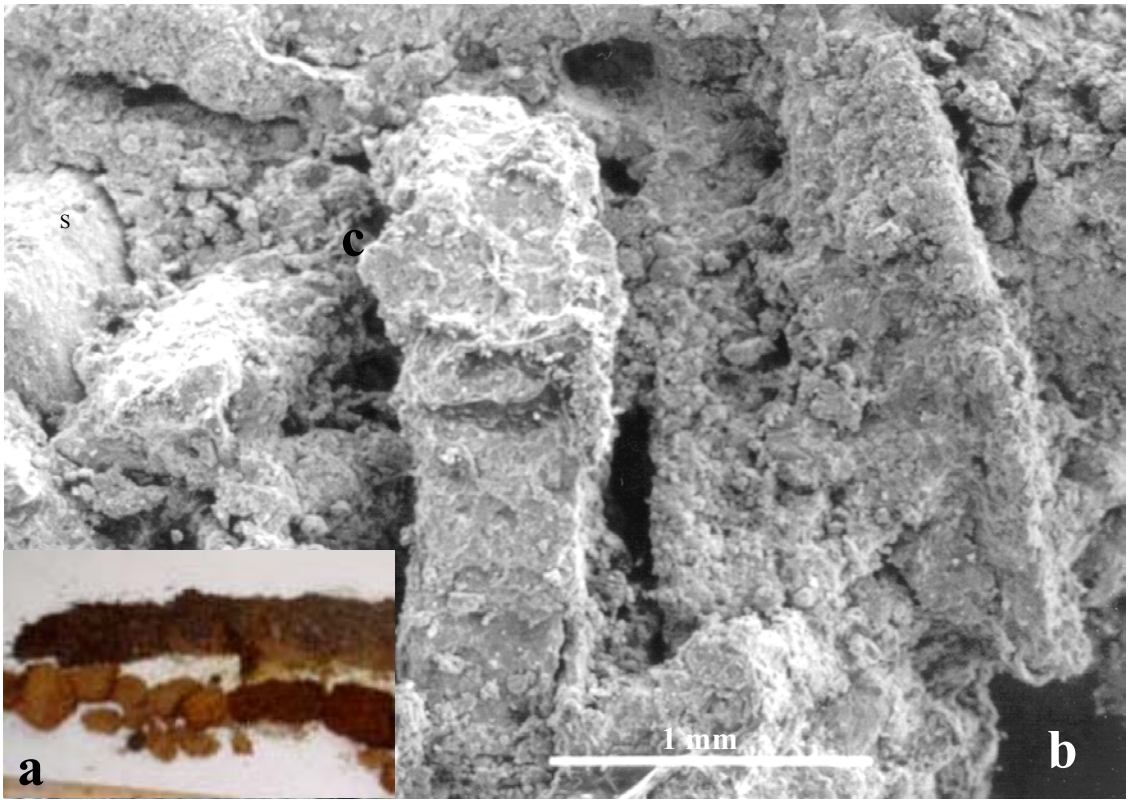

Figure 18. Photomicrographs showing (a) cemented Fe^0 filings and (b) enlarged SEM image of (a).

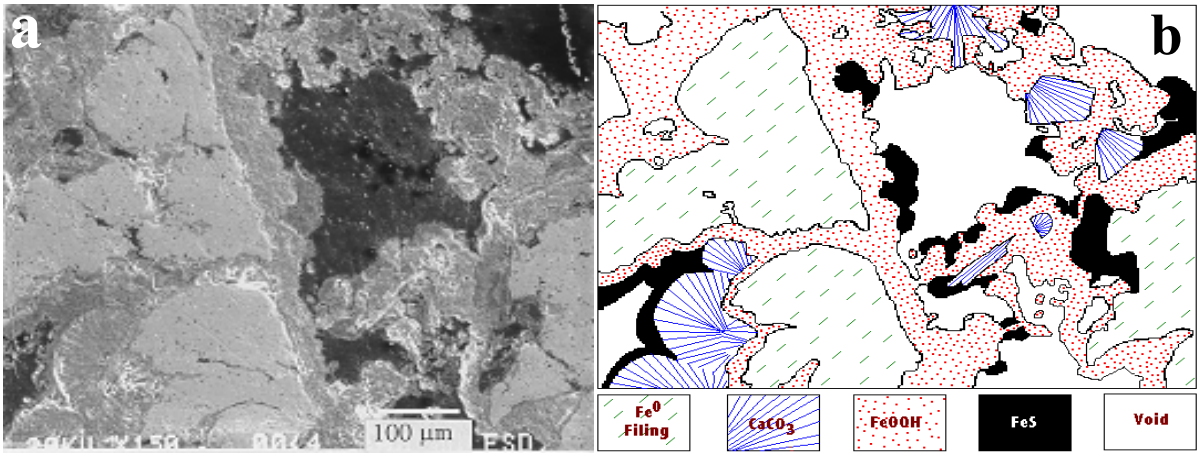

Figure 19. (a) Polished cross-section of cemented Fe^0 filings as shown in Figure 17 and (b) the outline of (a) showing Fe0 filings bound together by iron oxyhydroxides and aragonite coated with amorphous FeS (from Phillips *et al.* 2000).